Low-Thrust Enabled Highly Non-Keplerian Orbits in Support of Future Mars Exploration

Malcolm Macdonald[1] Robert J. M^{c}Kay[2], Massimiliano Vasile[2],
Advanced Space Concepts Laboratory, University of Strathclyde, Glasgow G1 1XJ, United Kingdom

Francois Bosquillon de Frescheville[3]
European Space Operations Centre, European Space Agency, 64293 Darmstadt, Germany

James Biggs[2], Colin M^{c}Innes[4]
Advanced Space Concepts Laboratory, University of Strathclyde, Glasgow G1 1XJ, United Kingdom

The technology of high specific impulse propulsion systems with low thrust is improving, opening up numerous possibilities for future missions applying continuous thrust to force a spacecraft out of a natural Keplerian orbit into a displaced non-Keplerian orbit. A systematic analysis is presented as to the applicability of highly non-Keplerian orbits throughout the Solar System. Thereafter, two applications of such orbits in support of future high-value asset exploration of Mars are detailed: a novel concept for an Earth-Mars interplanetary communications relay, on which the paper largely focuses, and a solar storm warning mission. In the former the relay makes use of artificial equilibrium points, allowing a spacecraft to hover above the orbital plane of Mars and thus ensuring communications when the planet is occulted by the Sun with respect to the Earth. The spacecraft's power requirements and communications band utilized are taken into account to determine the relay architecture. A detailed contingency analysis is considered for recovering the relay after increasing periods of spacecraft propulsion failure, combined with a consideration of how to deploy the relay spacecraft to maximise propellant reserves and mission duration. For such a relay, a combination of solar sail and solar electric propulsion may prove advantageous, but only under specific circumstances of the relay architecture suggested. For highly non-Keplerian orbits the dynamics of the spacecraft is also briefly extended to consider the elliptic restricted three-body problem and the effects of orbit eccentricity.

[1] Advanced Space Concepts Laboratory, University of Strathclyde, Glasgow, UK, AIAA Associate Fellow.
[2] Advanced Space Concepts Laboratory, University of Strathclyde, Glasgow, UK.
[3] Future Studies Operations Concept Engineer, European Space Operations Centre, Human Spaceflight and Exploration Department, Darmstadt, Germany
[4] Advanced Space Concepts Laboratory, University of Strathclyde, Glasgow, UK, AIAA Member.

Nomenclature

a_{ref}	dimensional reference acceleration, equal to unit sail lightness number $= 5.93$ mms^{-2}
$\boldsymbol{a}_{gc}$	nondimensional required acceleration vector to balance gravitational and centrifugal force
$\boldsymbol{a}_{SEP}$	nondimensional acceleration due to SEP thruster
e	eccentricity of orbit of smaller primary in 3-body problem
f	true anomaly
G	gravitational constant
I_{SP}	specific impulse
m	spacecraft mass
m_1	mass of larger primary
m_2	mass of smaller primary
$\boldsymbol{n}$	thrust vector orientation
p	semi-latus rectum of ellipse
$\boldsymbol{r}$, r	position vector with respect to centre of mass of primaries, orbit radius
T	continuous and constant low thrust
v	centripetal potential
V	augmented potential
α	pitch angle
β	solar sail lightness number
Δv	change in velocity
Δv_e	change in velocity, in ERTBP
λ	ratio of $\|\|\boldsymbol{a}\|\|$ to $\|\|\nabla \boldsymbol{V}\|\|$
μ	reduced mass gravitational parameter
ρ	distance between the two primary masses
$\boldsymbol{\omega}, \omega$	orbital angular velocity

I. Introduction

The concept of counter-acting gravity, and altering a spacecraft's trajectory from a natural free-fall path through the use of continuous propulsive thrust, was apparently first proposed by Dusek in 1966 [1] to generate artificial equilibria near the classical Lagrange points. This concept has since become known as a highly non-Keplerian orbit (NKO) and has been extensively studied to establish the fundamental dynamics of the problem [2].

In the late 1970s/early 1980s, Driver [3] outlined one of the first applications of a highly non-Keplerian orbit. Driver considered a spacecraft that would hover directly above the poles of the Earth for an extended period of time. Such a PoleSitter concept would be enabled by continuous thrust, where the thrust direction was always such that the spacecraft remained at a fixed distance along the polar axis. Subsequently, Forward considered using a solar sail to displace a body north or south of the geostationary ring [4, 5], around a decade after Farquhar had previously considered using a small solar sail to stabilize motion near the classical L_1 point in the Earth-Moon system [6]. It is of note that despite criticism of Forward's solar sail enabled displaced geostationary orbit concept, it has recently been validated by Baig and M^{c}Innes [7].

M^{c}Innes collated a significant wealth of material on solar sailing and highly non-Keplerian orbits [8], and the study of solar sail-enabled artificial displaced Lagrange points was considered extensively by NASA/JPL/NOAA under the GeoStorm mission concept [9, 10]. In addition to highly non-Keplerian orbits for solar sails, where the concept was largely developed, large families of orbits are also found to exist for spacecraft equipped with other forms of low-thrust propulsion, such as solar electric propulsion, SEP [2].

Large families of displaced orbits for a generic continuous low-thrust propulsion were first rigorously detailed by M^{c}Innes [11, 12], generated by considering the dynamics of the problem in a rotating frame of reference. As the angular velocity of the frame of reference is used as a free parameter of the problem, the orbits can be classified into families defined by the functional form taken by the angular velocity. In particular, the required thrust induced acceleration can be minimized by an optimum selection of the angular velocity.

The initial work led by M^{c}Innes has since been studied by others, e.g. Morimoto et al. [13,14], to develop the concept further, as such orbits could have a diverse range of potential applications. However, such work has mainly focused on Earth-centered trajectories - although some authors have considered individual applications of non-Keplerian orbits outside the Earth's influence. For example, the in-situ observation of Saturn's rings has been considered by, for example, M^{c}Innes [12] and Spilker [15]. In other work, Sawai, Scheeres & Broschart analyzed the control of a spacecraft hovering over a rotating body such as a comet or asteroid [16].Broschart & Scheeres [17] extended this work in the first instance by considering the case of using continuous control thrust to hover above an asteroid, and investigating the stability of realistic hovering control laws in both the body-fixed and inertial

reference frames, as well as presenting a case study of hovering above Asteroid (25143) Itokawa (which was the target of the Hayabusa mission).

In this paper, systematic consideration is given to all the families of non-Keplerian orbits, at a number of bodies in the Solar System to identify new regions of application and interest. Subsequently, the application of highly non-Keplerian orbits in support of future Mars exploration using near to mid-term technology is developed. Two Mars exploration support applications are detailed, where the objective is to outline the underlying astrodynamics, such that detailed mission budgets and timelines are beyond the scope of the paper. These two missions are a Mars communication relay, called The Sojourn Relay, and a solar storm warning mission called AreoStorm. Specifically, the scenarios presented are envisaged to support Mars exploration by high-value assets either in-orbit about Mars, or on the surface, where such high-value assets could be either human or robotic.

II. Highly Non-Keplerian Orbit Model and Definition

Overview

Families of periodic highly non-Keplerian orbits are quite different from open spiral trajectories used for spacecraft orbit transfer. They are obtained by considering the dynamics of the low thrust spacecraft in a rotating frame of reference, where the angular velocity of rotation of the frame of reference is used as a free parameter of the problem. Stationary solutions to the equations of motion are then sought in this rotating frame of reference, which correspond to periodic, displaced orbits when viewed from an inertial frame of reference.

As discussed in [2], trajectories that make use of a continuous thrust to offset gravity can be divided into two categories. The first category is the displacement of 2-body orbits – for example, the displacement of the geostationary ring above the "traditional" ring, which is within the equatorial plane. In this case large families of orbits are found, parameterized by the angular velocity of the rotating frame of reference, and regions of linearly stable orbits can be identified. The second category of displaced orbits is the displacement of 3-body equilibrium solutions. While displaced orbits with a free orbit period may be generated for 2-body systems, a set of artificial equilibrium points are generated for 3-body systems when the angular velocity of rotation of the frame of reference is chosen to be that of the two primary masses. As the region in which the equilibrium solution is sought moves away from the second body in the 3-body problem, the 2 and 3-body problems match asymptotically, with the proviso that the orbit period remains fixed to that of the secondary body.

Model

By following M^{c}Innes [23, 18], the conditions for circular displaced highly non-Keplerian orbits can be investigated by considering the dynamics of a spacecraft of mass m in a reference frame $\boldsymbol{R}(x, y, z)$ rotating at constant angular velocity $\boldsymbol{\omega}$ relative to an inertial frame $\boldsymbol{I}(X, Y, Z)$. The rotating reference frame, $\boldsymbol{R}(x, y, z)$, uses Cartesian coordinates, where the x-axis points between the primary masses, the y-axis denotes the axis of rotation and the z-axis is orthogonal to both, as shown in Fig. 1.

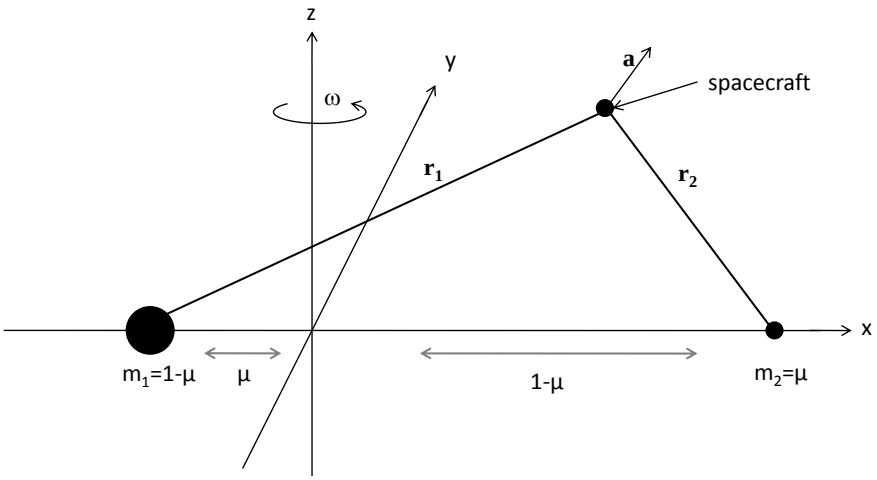

Fig. 1 The rotating coordinate frame and the spacecraft position therein for the restricted three-body problem

With such a system the equations of motion of the spacecraft are given by,

$$\ddot{\boldsymbol{r}} + 2\boldsymbol{\omega} \times \dot{\boldsymbol{r}} + \nabla \boldsymbol{V} = \boldsymbol{a} \tag{1}$$

where, $\boldsymbol{r}$ is the position vector of the spacecraft from the primary body, dots denote differentiation with respect to time t, and $\boldsymbol{V}$ and $\boldsymbol{a}$ are the augmented potential and the continuous and constant acceleration due to the propulsion system respectively, the former being given by,

$$V = -\left(\frac{1-\mu}{\|\boldsymbol{r}_1\|} + \frac{\mu}{\|\boldsymbol{r}_2\|}\right) + \frac{1}{2}\|\boldsymbol{\omega} \times \boldsymbol{r}\|^2 \tag{2}$$

in units where the gravitational constant $G = 1$ and the system has total unit mass, and where μ is the reduced mass,

$$\mu = \frac{m_1}{m_1 + m_2} \tag{3}$$

and the latter being given by,

$$\boldsymbol{a} = \left(\frac{T}{m}\right)\boldsymbol{n} \tag{4}$$

where, $\boldsymbol{n}$ is the direction of the thrust T. Note that Eq. (4) makes no assumption about the propulsion system used, so for a solar sail Eq. (4) must be modified accordingly. By setting $\ddot{\boldsymbol{r}} = \dot{\boldsymbol{r}} = 0$, i.e. assuming equilibrium conditions in the rotating frame, then the equation $\nabla \boldsymbol{V} = \boldsymbol{a}$ defines a surface of equilibrium points as illustrated in Fig. 2 for the immediate region around Mercury for a solar electric propulsion (SEP) spacecraft with acceleration of up to 0.3mms^{-2}, where, in Fig. 2, the assumption of the circular restricted three-body problem is made to simplify the dynamics of the system. Anywhere on this equithrust surface, a spacecraft with the required thrust, oriented in the direction needed, will therefore exist in equilibrium with the body in question.

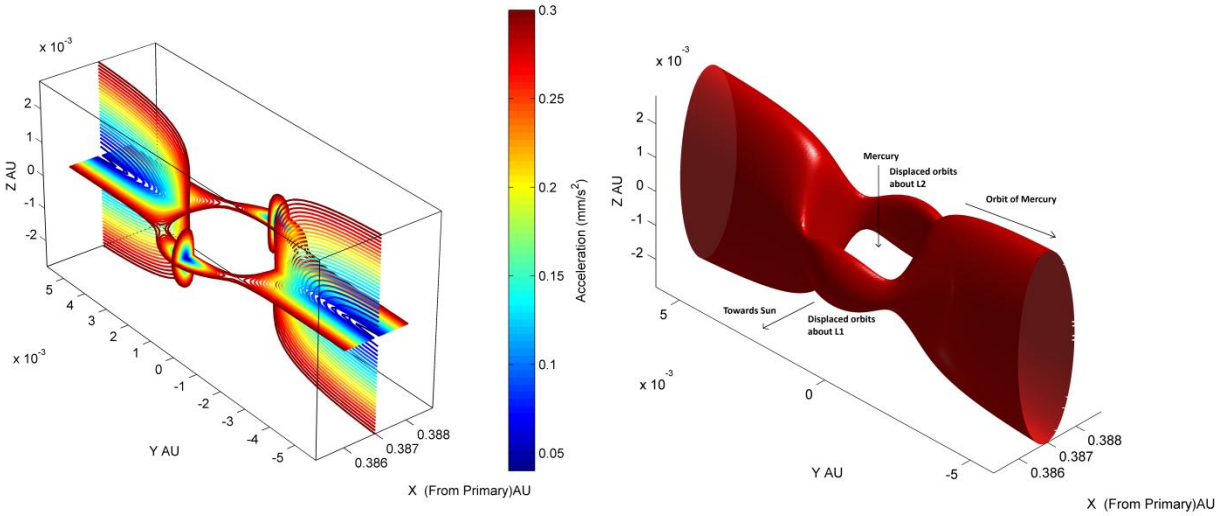

Fig. 2 Artificial equilibrium points for the Sun-Mercury L_1/L_2 system depicted by equithrust contours projected onto the planes perpendicular to and parallel to the orbital plane (left), and the equithrust surface equivalent to an acceleration of 0.3mms^{-2} (right).

The required thrust vector orientation for an equilibrium solution is determined by,

$$\boldsymbol{n} = \frac{\nabla \boldsymbol{V}}{\|\nabla \boldsymbol{V}\|} \tag{5}$$

and the magnitude of the thrust vector, $\|\boldsymbol{a}\|$, is given by,

$$\|\boldsymbol{a}\| = \|\nabla \boldsymbol{V}\|. \tag{6}$$

With these conditions the spacecraft is then stationary in the rotating frame of reference, tracing out an orbit in the inertial frame. As discussed in [2], Eq. (6) provides a simple definition of what constitutes a highly non-Keplerian orbit. Defining a parameter λ such that,

$$\lambda = \frac{\|\boldsymbol{a}\|}{\|\nabla \boldsymbol{V}\|} \tag{7}$$

The specific case of highly non-Keplerian orbits can be considered, that is, when $\lambda \cong 1$, or, equivalently, when the acceleration applied by the low-thrust propulsion system is of approximately the same order as the gravitational acceleration experienced by the spacecraft. For comparison, orbits with $\lambda = 0$ represent ideal Keplerian orbits (for the 2-body problem, and free-fall orbits in the 3-body problem), essentially the large subset of classical orbital mechanics without the addition of a non-conservative force. Orbits with $\lambda \sim 0.1$ are effectively weakly-perturbed Keplerian orbits, and as such can be referred to as non-Keplerian orbits. There are numerous examples of such orbits in the literature: for instance, the considerable body of work which has considered the use of rather small solar sails to artificially precess elliptical orbits for space physics mission applications. Some examples of such work are that of Macdonald and M^{c}Innes' consideration of an ellipse being precessed if the sail is Sun-facing, leaving the orbit averaged semi-major axis and eccentricity unchanged [19]. By an appropriate choice of sail loading, the elliptical

orbit can be forced to precess at a Sun-synchronous rate, maintaining a science payload permanently within the geomagnetic tail, a concept utilized by the GeoSail mission [20, 21]. An even more recent example is the extended Sun-synchronous orbits proposed by Macdonald et al. [22]. It is worth noting that although these examples are of non-Keplerian orbits, they are a quite separate subset to that of highly non-Keplerian orbits which this paper focuses on.

Extension to solar sail case

Due to the orientation-constrained nature of solar sail propulsion, i.e. a sail cannot thrust towards the Sun, the family of highly non-Keplerian solar sail orbits can thus be thought of as limiting cases of the more general analysis for non-orientation constrained low thrust propulsion technologies discussed in the previous subsection. The simple form of Eq. (4) for the continuous and constant acceleration of the spacecraft is replaced by [23],

$$\boldsymbol{a} = \beta \frac{1-\mu}{r_1^2} (\hat{\boldsymbol{r}}_1 \cdot \boldsymbol{n})^2 \boldsymbol{n} \tag{8}$$

where, β is the sail lightness number, the ratio of solar radiation pressure acceleration to solar gravitational acceleration (fully defined in [8]), $\hat{\boldsymbol{r}}_1$ is the position vector of the spacecraft with respect to the Sun, and $\boldsymbol{n}$ is the unit normal to the sail, representing the thrust vector. McInnes [23] then considered the dynamics of the spacecraft in a rotating reference, as shown in Fig. 1. The solar sail lightness number required for equilibrium can be determined to be [23],

$$\beta = \frac{\mathrm{r}_1^2}{1-\mu} \frac{\nabla V \cdot \boldsymbol{n}}{(\hat{\boldsymbol{r}}_1 \cdot \boldsymbol{n})^2} \quad . \tag{9}$$

Using these equations the artificial equilibrium points available to a solar sail and a solar electric propulsion spacecraft of equivalent acceleration can be compared, as in Fig. 3; for the purposes of comparison, an SEP spacecraft is considered with acceleration equivalent to a solar sail with characteristic acceleration 0.3 mm s^{-2}.

As can be seen in Fig. 3, the advantage of SEP over the solar sail for this candidate orbit is that there are no forbidden regions (denoted by the filled areas) due to the orientation constrained nature of the solar sail, requiring that it thrusts away from the Sun – meaning that there are areas around both L_1 and L_2 which are accessible to an electric propulsion system that are not accessible to a sail. It can also be seen that, even where non-Keplerian orbits are possible with a sail, the region is much smaller as the sail can only bring a component of the acceleration required in the direction of the thrust direction arrows, unlike the SEP system.

Having defined what constitutes a highly non-Keplerian orbit, and illustrated the potential families of such orbits, it is possible to catalogue the domain of these orbits for the various celestial bodies in the solar system for different propulsion systems. For more specific examples of such plots, see M^{c}Kay et al. [24]. In this paper, applications of some of these orbits in support of future high-value asset exploration of Mars are discussed at length. These opportunities concepts were selected for study by consideration of the benefits and drawbacks of enabling highly

non-Keplerian orbits via both SEP and solar sailing, at various Solar System bodies – a summary of which is given in Table 1.

From Table 1 it is seen that highly non-Keplerian orbit opportunities about Earth and Mars offer the best cost – reward ratio from a practical perspective, allowing a usefully large domain of highly non-Keplerian orbits for both SEP and solar sail near-term technologies, whilst providing a sufficiently high photon flux to allow both forms of propulsion to perform well. It is thus prudent to consider applications of highly non-Keplerian orbits about these two bodies in the first instance as further from the Sun there is insufficient photon flux for either the SEP or sail to function particularly well. Bodies closer to the Sun may provide some useful opportunities, but the gravitational potential well is deeper, reducing the size of the orbit domain in a like-for-like comparison for SEP spacecraft. However, it is noted that the close proximity to the Sun delivers a significantly increased solar sail thrust magnitude which can hence offset some of these potential drawbacks. The sail will however need to withstand high film temperatures, and of course the orbit domain is fundamentally limited due to the inability to thrust towards the Sun. Finally, it is noted that the use of a suitable nuclear power source would eliminate many of the power constraint issues detailed in Table 1. However, the system mass could potentially be increased so much by a nuclear reactor as to simply offset any potential gains and equally limiting the acceleration magnitude.

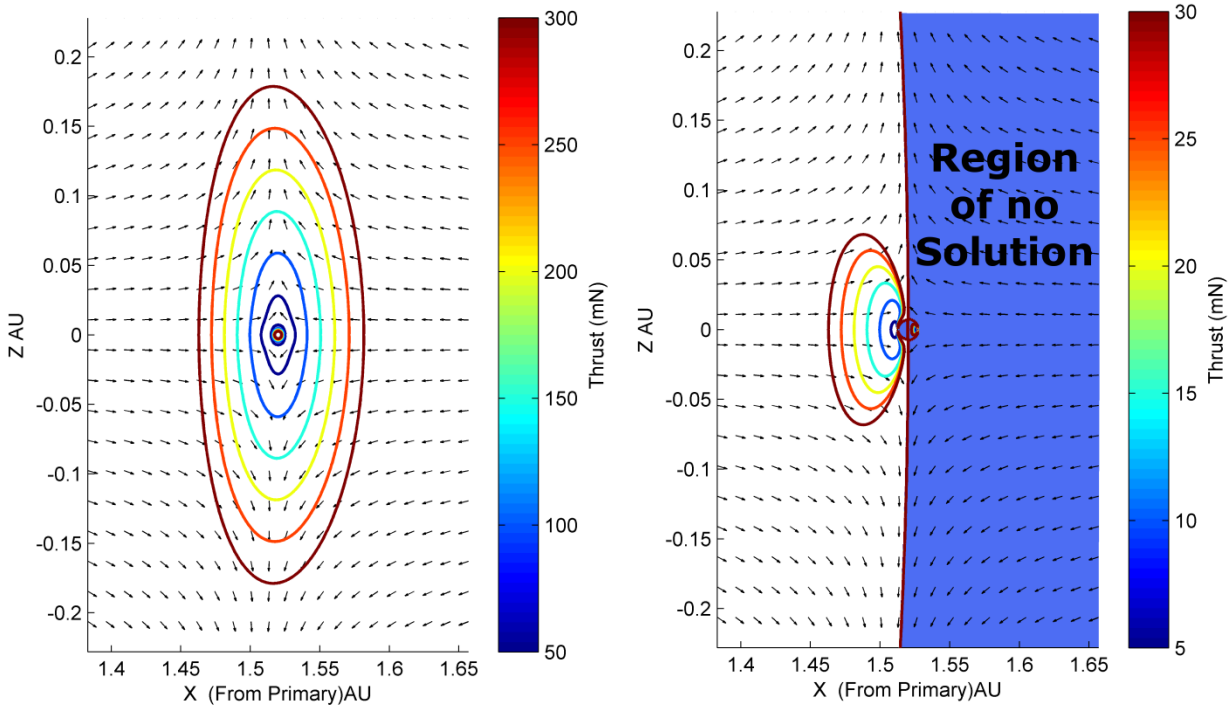

Fig. 3 Non-Keplerian orbit equithrust contours projected onto the plane perpendicular to the orbital plane for the Sun-Mars-spacecraft 3-body system for SEP spacecraft (left) and solar sail (right) of equivalent acceleration. Filled in area on solar sail plot is where no solution is possible.

Table 1: Potential of non-Keplerian orbits (NKOs) throughout the Solar System

Body	Three-Body NKOs		Two Body NKOs		Propulsion System Comment
	Advantages	**Disadvantages**	**Advantages**	**Disadvantages**	
Mercury	Close to the Sun gives good power availability	Deep inside Sun's gravity well and small planet; limits orbit domain	Relatively small central body	Very difficult to get into orbit and few applications	Good power for SEP, relatively large orbit domain for a sail, temperature issues
Venus	Close to the Sun gives good power availability	Deep inside Sun's gravity well but Earth-size planet; limited orbit domain	Good science applications; see [2]	Relatively large central body, close to Sun limits feasible orbits within sphere-of-influence	Good power for SEP, relatively large orbit domain for a sail, benign environment for spacecraft
Earth	Good balance: close to Sun for power but not being too deep into Sun's gravity well	Still requires a significant amount of thrust to occupy useful orbit.	Good science and commercial applications; see [2].	Relatively large central body, close to Sun limits feasible orbits within sphere-of-influence	Good power for SEP, fair environment for a sail, easy to get to and benign environment
Moon	Enables continuous communication with Lunar poles	Heavily biased mass ratio towards Earth limits orbit domain	Relatively small central body	Proximity to Earth limits feasible orbits within sphere-of-influence	Good power for SEP, complex Sun-line tracking for sail, benign environment
Mars	Distant from Sun, allows significant orbit domain	Moons may provide issues regarding orbit stability, but no major disadvantages	Relatively small central body, distant from Sun - enables feasible orbits within sphere-of-influence	No obvious disadvantages	Limited power for SEP must be considered, sail orbit domain limited
Ceres	Very small central body allows close proximity	Difficult to get to from Earth in comparison to Venus and Mars	Relatively small central body enables large displacements	Difficult to get to	Limited power for SEP and low solar flux levels
Jupiter/ Saturn	Very large mass of planet & distance from Sun effectively reduces to 2-body problem	Difficult to get to from Earth in comparison to Venus and Mars	Distant from Sun enables feasible orbits within sphere-of-influence at for example the rings of Saturn	Difficult to get to	Very limited power for SEP, and sail orbit domain is negligible

III. A Novel Interplanetary Communications Relay – The Sojourn Relay

A novel application of highly non-Keplerian orbits is for a future Earth-Mars communications relay. This idea is not dissimilar in concept to that proposed for lunar communications by Wawrzyniak & Howell [25], and other authors who have noted that the problem of solar occultation can be avoided using displaced orbits, such as M^{c}Innes & Simmons [26], and Simo & M^{c}Innes [27], and was introduced briefly in Ref. [24].

An Overview of The Sojourn Relay

For any future high-value asset Mars exploration, such as a human crew or a high-value Unmanned Autonomous System such as an advanced rover or aerial explorer, continuous communication between the surfaces of the two planets will be required. Currently, during periods of solar occultation, assets both in-orbits about Mars and on its surface are out of communication with the terrestrial ground segment. While such a scenario is undesirable for current generation robotic assets, it is acceptable. However, this is not so for human exploration. Therefore, a communication relay is required to ensure continuous communication between Earth and Mars during this period, the new architecture proposed is termed Sojourn to reflect the temporary nature of this driving requirement. To address this issue, non-Keplerian orbits above or below the orbital plane of Mars are suggested as a means of enabling such a relay. Indeed, it is noted that any spacecraft within, or even which passes through, the orbital plane of a planet in the solar system shall experience periods of solar occultation of Earth, and thus the problem is more generic than the specific case of Mars.

A schematic diagram of the architectural options of such a relay is shown in Fig. 4, where the angle X represents the field-of-view exclusion zone about the Sun as viewed from Earth, and angle Y is the equivalent spacecraft-Mars-Sun angle. The technology requirements of such an array are largely determined by the field-of-view exclusion zone about the Sun, which is dependent on how close to the limb of the Sun radio signals can be transmitted without interference from the solar plasma. For design optimization purposes a spacecraft in proximity of Mars is preferred, as the long slant range back to Earth can be compensated for through the use of a large Earth-based antenna, while a spacecraft in proximity of Earth would require such a large antenna on-board the spacecraft, or on Mars.

Consider the assumption of a 4-degree field-of-view exclusion of Mars from Earth. This is a realistic value if assuming X-band communications, however it is noted that Morabito and Hastrup [28] suggest reasonable data returns as low as 2.3 degrees in X-band, provided that the effects of any possible significant solar transient events are neglected. Furthermore, different electromagnetic communication bands, such as Ka-band, define different field-of-view exclusion angles, however this point will be returned to in the next subsection.

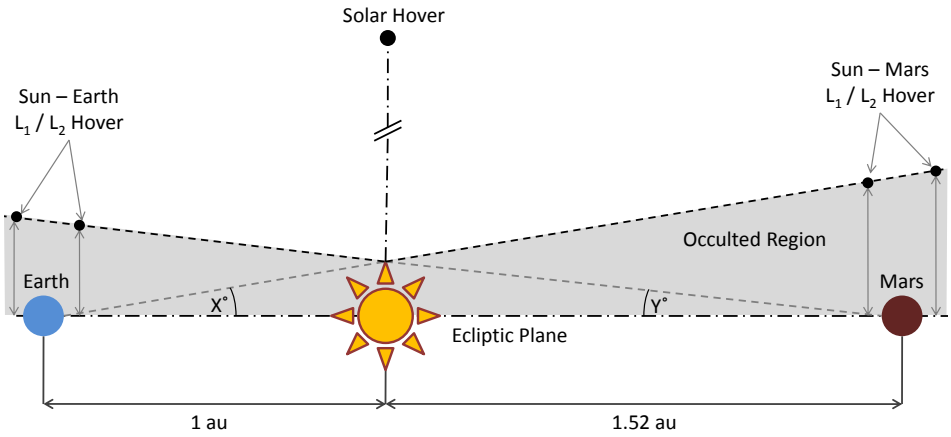

Fig. 4 Earth-Mars communication relay architecture options out of the orbital plane.

With such an angle the Sun – Mars stations can be determined to be located approximately 0.176AU out of the orbital plane, while the Sun – Earth stations can be determined to be located approximately 0.116AU outside the orbital plane, since the equivalent spacecraft-Mars-Sun angle is then 2.64°. The much shallower gravitational potential well at Mars significantly increases the distance from the planet that a spacecraft can hover in direct comparison to Earth.

An interesting extension to this concept is to consider spacecraft in orbits displaced out of the orbit plane of Mars and either leading or trailing Mars. Considering the symmetry of Fig. 4, the field-of-view exclusion defines a conic region around the Sun where Mars is hidden from the Earth. If this conic region is considered end-on from behind Mars, as shown in Fig. 5, as well as achieving continuous communications by displacing a spacecraft directly above Mars, a spacecraft could also be displaced onto the circular, when projected in two dimensions, region around Mars defined by the field-of-view exclusion, so that one spacecraft was trailing and the other leading the orbit of Mars.

Naturally, as the two spacecraft track Mars they too will enter the blackout region. As depicted in Fig. 5, the leading spacecraft will move beyond the edge of the blackout region as the trailing spacecraft moves into this region. However, the separation of the two spacecraft means that only one will ever be in this region at any given time, and, given the distance between the spacecraft, the arc of the orbit is easily sufficient to maintain a line-of-sight between the two spacecraft, i.e. one will not be occulted by Mars with respect to the other, allowing continual communications to be achieved by relaying the signal from the occulted spacecraft to the one outside the occulted region and then on to Earth.

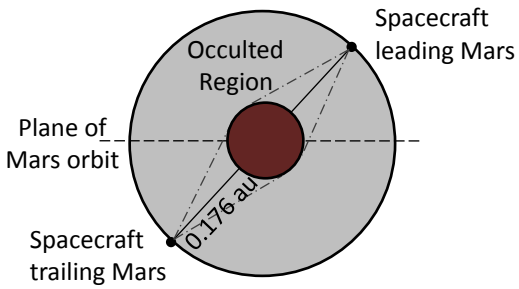

Fig. 5 End-on view of an alternative Mars-Earth communication relay architecture option, looking along the orbital plane.

Positioning of the spacecraft then depends on what is required from the mission. The relay spacecraft will need less thrust to maintain their position with respect to Mars if they are not maximally displaced out of the orbital plane, but reducing this displacement increasingly limits communication capabilities to assets near the equator of Mars. To communicate with assets at higher latitudes, particularly the scientifically interesting polar regions, it will be necessary to displace the spacecraft out of the orbital plane.

Relay Using Purely Solar Electric Propulsion

Having outlined the concept of the relay, the amount of thrust required in order to occupy some potential hover points to enable the relay is quantified. To do this a SEP thruster with a maximum thrust of 300mN and a specific impulse (I_{SP}) of 4500 seconds is assumed: these assumptions allow for a consideration of opportunities based on current or near-term technology, such as the QinetiQ T6 thruster, which will theoretically provide a thrust of up to 230 mN at an I_{SP} of above 4500 seconds for the BepiColombo mission [29]. To provide a benchmark for the study the spacecraft mass was simply assumed to be 1000kg, thus defining the acceleration capability of the spacecraft to be of up to 0.3 mm s^{-2}.

Considering first of all the non-Keplerian orbit regions displaced out of the orbital plane, as illustrated in Fig. 3, it can be seen that a 300 mN thrust is sufficient to displace the spacecraft 0.176AU directly above Mars. This is just enough to ensure that the spacecraft could communicate with Earth, assuming a 4 degree field-of-view exclusion, although clearly this is the bare minimum clearance required and thus leaves no margin. However, there are some advantages to considering the dual spacecraft option discussed in the previous subsection, over the case of a single spacecraft hover. Firstly, hovering directly above Mars limits communications to just the polar region. If the spacecraft are trailing or leading the orbit then communication with the equatorial regions is enabled, with the ability to cover most of both hemispheres of Mars. A more important advantage can be shown by considering the equithrust contours in the plane illustrated by Fig. 5, i.e. the *y*-*z* plane, as shown in Fig. 6.

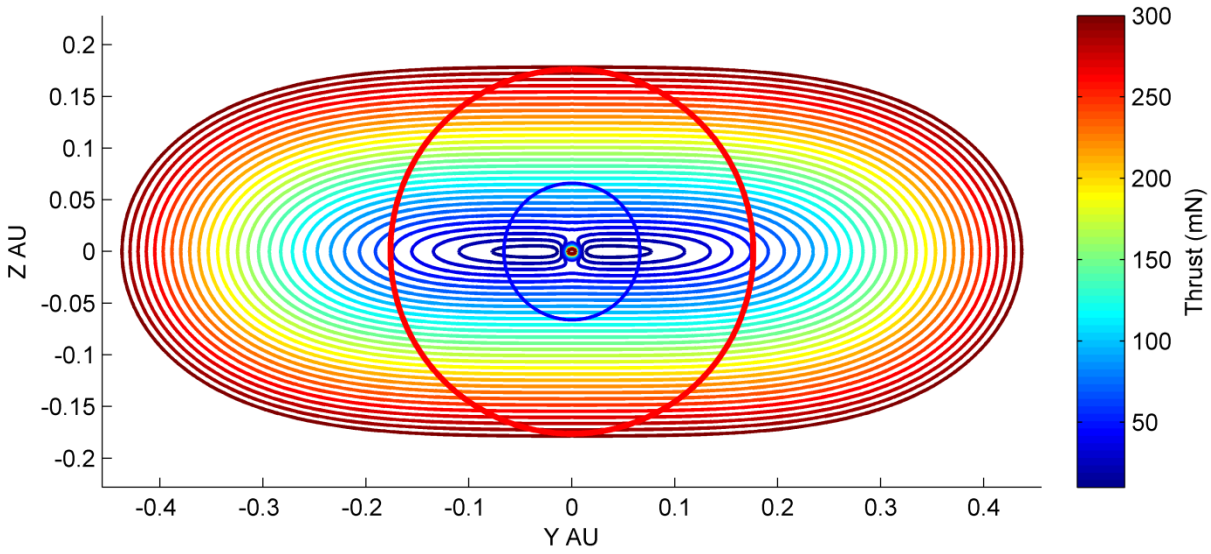

Fig. 6 An end-on view of NKO depicted by equithrust contours, for a 1000kg SEP spacecraft about Mars, looking along the orbital plane. The outer heavy and inner light circles indicate the field-of-view exclusion zone for X and Ka-band communications respectively.

As can be seen in Fig. 6 it is much easier to displace the spacecraft orbit from Mars in this plane (i.e. along *y*) than out of it (i.e. along *z*) and so a spacecraft can occupy a non-Keplerian orbit on the surface defined by the field-of-view exclusion for less thrust if it trails or leads Mars rather than hovering directly above. For example, displacing the spacecraft 45 degrees out of the orbital plane of Mars would reduce the thrust requirements to approximately 200 mN, assuming the 4 degree field-of-view exclusion defined by X-band communication. So, practically, it may be more feasible to maintain the communications relay using two spacecraft with lower thrust than a single spacecraft which needs higher thrust.

This is true for the case of a 4 degree field of view exclusion of Mars from Earth by the Sun, which is a realistic value if it is assumed that the communication relay is via the X-band portion of the electromagnetic spectrum. If instead the use of Ka-band is considered, the field of view exclusion can be reduced to just 1.5 degrees, as shown in Fig. 6, as signals in this frequency range are less affected by the solar plasma. This obviously reduces the thrust requirements for the relay spacecraft considerably: it would then need to hover 9.872 million km (0.066 AU) directly above Mars, which could be done for a one tonne spacecraft with approximately 110mN of thrust, or there could be two spacecraft (one leading and one trailing the orbit of Mars, as in Fig. 5) displaced 45 degrees out of the orbital plane (6.98 million km above Mars' orbital plane), which would require just 80 mN of thrust each. Ka-band would be preferable for many other reasons, for example the higher bandwidth and thus data rate that comes with it, and the lower power requirements for the antenna, but Ka-band communication is technologically more challenging than that of X-band and is thus more expensive and less readily-accessible as an option. However, NASA is already beginning the process of transitioning to Ka-band due to the many potential advantages it offers with the Mars Reconnaissance Orbiter being equipped with a fully functioning Ka-band communications suite [30].

It should also be considered that the non-Keplerian orbit actually need only be maintained during periods of solar occultation, and hence it may be possible to extend the spacecraft lifetime by only using the thrusters to provide significant amounts of thrust during such periods and allowing the spacecraft to follow a conventional near-Keplerian orbit during other periods; hence the name The Sojourn Relay. However, continuous displacement may be attractive to ensure continuous communication with assets at the polar regions at the expense of total mission lifetime. For example, the synodic period of Mars with respect to Earth and the Sun (and thus the occultation repeat period) is approximately 780 days on average, although it varies due to the eccentricity of the orbit of Mars. The actual duration of the communications blackout caused by solar conjunction varies from mission to mission depending on various factors, such as the amount of link margin designed into the communications system, the minimum data rate that is acceptable from a mission standpoint, as well as the exact Sun-Earth-Mars alignment. In addition, the level of solar activity will be a factor, with highly energetic events such as solar flares or coronal mass ejections adding to the general background level of signal disruption - with, conversely, a quiescent Sun during a period of solar minimum activity proving advantageous in such situations. Gangale [31] summarized the communications outage periods for six different recent Mars missions, showing that the average outage period is of the order of one month, although there is a reasonable spread as evidenced by comparison of the approximate 40 days of blackout experienced by the Viking 1 orbiter during the 1976 conjunction and the approximate 18 days of blackout encountered by Mars Global Surveyor in 2004.

Bearing this in mind, it can be envisaged a mission that would see the SEP spacecraft thrusting to hover above Mars for a certain number of days to maintain communications whilst Mars is occulted, and then, when Mars is no longer occulted, using the thruster efficiently to re-acquire the relevant artificial equilibrium point (AEP) via a pre-planned orbital maneuver, returning to the correct point for the next occultation of Mars, where the thruster would then be switched back on to occupy the non-Keplerian orbit position again. Thus, the spacecraft would only need to continually thrust at the levels outlined previously for perhaps only a few weeks in every 2.13-year period (approximately) as opposed to the entire time, which would significantly extend the on-station time as allowed by the thruster propellant reserves.

Finally, it is worth considering the advantages of such a communications relay architecture option, over some of the more obvious potential architectures. Consider a relay consisting of a spacecraft at Earth's L_4/L_5 point, or likewise at Mars' L_4/L_5 point. The former case of an Earth-Earth L_5-Mars relay then requires that a signal be sent over a total distance of approximately 3.21AU, with a distance of about 2.21AU between Mars and the relay spacecraft. The latter case of an Earth-Mars L_4-Mars relay spans a distance of approximately 3.73AU, with a distance between Mars and the relay space of around 1.52AU. Compare these numbers with the architecture offered by a Mars proximity AEP, with the relay spacecraft about 0.18AU from Mars and a total relay distance of around 2.7AU, meaning that the non-Keplerian orbit allows a relay station that spans a considerably smaller distance than using conventional Lagrange points, and enables a considerably higher data rate between the surface of Mars and the relay spacecraft.

As noted by Strizzi et al. [32], the size and power of the equipment needed for these distances make the L_4 and L_5 locations unrealistic for relay stations, although the inherent stability of these regions is beneficial in terms of station-keeping.

Relay Using Hybrid Solar Electric Propulsion / Solar Sail

Both SEP and solar sail low thrust propulsion systems have their own advantages and disadvantages. Solar sailing has the advantage that it requires no propellant, and thus can maintain continuous low thrust indefinitely, although in practice, long-term degradation of the optical surface may reduce the efficiency of the sail and propellant may be required for attitude control [33]. However, with SEP the thrust can be oriented in any direction, allowing access to artificial equilibria that a solar sail would be forbidden from with its inherent inability to thrust in the direction towards the Sun. Thus, in principle there is a strong case for studying a device that would combine the best features of both systems, to obtain a hybrid sail. Indeed, it has recently been suggested that such an approach may, in recognition of the high Advancement Degree of Difficulty of solar sailing, that is to say the difficulty of progressing solar sailing from one technology readiness level to the next, be the best means of advancing solar sail technology [34]. Such a propulsion concept has been considered in the literature previously, see, for example Leipold & Götz [35] and Mengali & Quarta [36], with the latter showing that hybrid sails have the attractive feature of reducing mission times for heliocentric transfers when compared to both the equivalent pure sail and pure SEP trajectories. Recently, Baig & M^{c}Innes [37], Simo & M^{c}Innes [27] and Ceriotti & M^{c}Innes [38] have all considered the case of displaced highly non-Keplerian orbits for a hybrid sail in the Sun-Earth and Earth-Moon 3-body systems for observation and communications applications.

The analysis of [37] is followed by considering a partially reflecting hybrid sail consisting of an SEP thruster attached to the centre of a solar sail, a model adapted from that of Leipold & Götz [35]. The solar sail is taken to be square, with part of the sail area at the centre of the sail covered by flexible thin film solar cells (TFSC), which act as a power source for the SEP system.

The acceleration vector $\boldsymbol{a}_{gc}$ required to cancel the gravitational acceleration of the two primary masses and the centripetal acceleration in the rotating reference frame, allowing an artificial equilibrium point $\boldsymbol{r}_0$ to be occupied, can be achieved with a hybrid sail through the vector sum of the solar radiation pressure and SEP acceleration vectors. The combination of acceleration from both solar sail and SEP can be thought of as modifying Eq. (6), giving,

$$\nabla V(\boldsymbol{r}_0) = \boldsymbol{a}_S + \boldsymbol{a}_{SEP} \triangleq \boldsymbol{a}_{gc} \ . \tag{10}$$

Ref. [37] showed that it is possible to orient the solar radiation pressure acceleration vector in order to obtain all or at least part of the acceleration vector $\boldsymbol{a}_{gc}$ required to occupy an AEP at $\boldsymbol{r}_0$, since, for a pure solar sail or pure SEP system the required acceleration magnitude and thrust orientation are completely defined by the location of the AEP. Baig & M^{c}Innes [37] proceed by selecting this optimum orientation to obtain the maximum benefit from the solar sail, and then use this acceleration to minimize the SEP thrust to achieve the desired vector $\boldsymbol{a}_{gc}$. Here, though,

instead it is assumed that the thrust from the SEP system is initially used to achieve all of the vector $\boldsymbol{a}_{gc}$, allowing the spacecraft to occupy a given artificial equilibrium point. Then, added to that is the magnitude of the acceleration from the solar sail oriented such as to maximize thrust along the vector $\boldsymbol{a}_{gc}$, as now defined at the displaced AEP. This allows an examination to be performed as to the potential gains of adding a solar sail to a SEP spacecraft, rather than vice-versa, and recognizes the relative technical maturity of the two technologies. It should hence be stated that such a hybrid is not an exact like-for-like comparison with the hybrid of Baig & M^{c}Innes, as by definition the approach taken in this paper has greater acceleration available to it, and to truly compare the performances of the two an equal mass budget would have to be defined for each spacecraft. Likewise, in regions where the solar sail is effective, the hybrid has a greater magnitude of acceleration available to it compared to the pure-SEP system, allowing access to AEP that would otherwise be beyond the capabilities of the pure SEP system with thrust equal to that of the SEP part of the hybrid SEP/solar sail spacecraft, but again the comparison is inexact unless spacecraft of equal mass are compared.

With this in mind the analysis considered for a pure-SEP system, in determining the non-Keplerian orbit equithrust contours at Mars, can be repeated for the hybrid sail. In this analysis it is assumed that the hybrid spacecraft has a solar sail of characteristic acceleration 0.2 mms^{-2} (equivalently, sail lightness number of 0.034) and sail reflectivity 0.9, the sail area is thus 45m × 45m, giving a sail loading of 45.63 gm^{-2}. The TFSC reflectivity is taken to be 0.4 and the TFSC area is 12 m^2. This sail is assumed to be attached to a 1000 kg SEP-propelled spacecraft capable of a maximum thrust of 300mN, as assumed previously. It is found that adding a solar sail to the SEP spacecraft allows access to a greater volume of space for non-Keplerian orbits: specifically, there is a reasonably large increase of available non-Keplerian orbits on the day-side of the planet around L_1 and a small increase on the night-side of the planet around L_2. This asymmetry is to be expected, given the regions of non-Keplerian orbits the pure sail can access. It is also found that the addition of the solar sail does not allow the hybrid to be displaced any further out of the orbital plane for the same amount of thrust, and thus in the context of the Earth-Mars communication relay as described previously this is perhaps a disappointing result. However, deeper consideration of the solar sail reveals why both of these points are indeed the case.

Firstly, consider the artificial equilibrium solutions for the solar sail itself. M^{c}Innes [39] considered the equilibrium solutions for a non-perfect solar sail (which is of importance because, aside from reducing the magnitude of the solar radiation pressure exerted on the sail surface, the partial reflectivity and hence finite absorption means that the radiation pressure force vector is no longer normal to the sail surface), showing that the equilibrium surfaces and accessible regions are slightly different, and that for a non-perfect reflectivity, there are no regions of possible solutions directly above the planet. Thus, it is impossible to have a solar sail stationed at a hover point directly above the planet. Even regardless of the reflectivity this is effectively the case: for a perfectly reflecting sail there is a region of singularity above the Earth where a sail would have to have effectively infinite acceleration in order to occupy such a spot [39]. Bearing this in mind it is not surprising, therefore, that the hybrid sail shows no advantage over the pure SEP system for non-Keplerian orbits displaced directly above the planet. Regardless, the fact that there

is no advantage in using a hybrid to hover directly above Mars does not in itself rule out the possibility of a hybrid system being potentially more useful than SEP alone as part of such a communications relay. Hovering directly above Mars is not exactly the same as a polesitter spacecraft, i.e. a spacecraft constantly aligned with the polar axis, due to the tilt of that axis, as illustrated in Fig. 7 for the 25.2 deg. axial tilt of Mars. Four specific points of interest are highlighted in Fig. 7 which illustrate where the spacecraft can be stationed such that they are directly above the pole of Mars.

Three of these points are on the day-side of Mars: the first two points show that the addition of the solar sail component of the hybrid extends the distance the spacecraft can hover directly above the pole at the summer solstice from 0.114AU to 0.137AU (i.e. can now station at the former point as opposed to the latter), or, equivalently, to occupy the latter point the hybrid spacecraft needs a thrust of only 240mN from the SEP component, compared to the 300mN required for a pure-SEP spacecraft. The third point shows the minimum distance required to complete the communications relay in Ka-band, which requires approximately 130mN from the hybrid SEP and 190mN from the pure-SEP. The fourth point on the night-side of the planet shows that having the sail is of no additional benefit here.

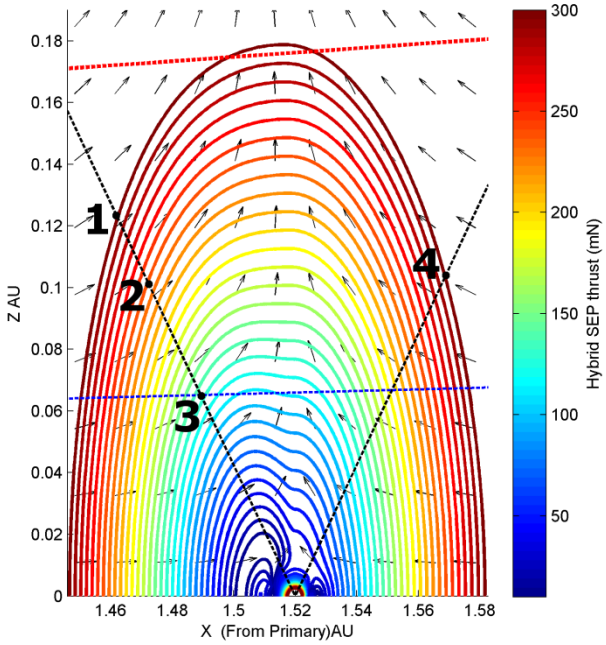

Fig. 7 NKO equithrust contours at Mars, projected onto the plane perpendicular to the orbital plane, for a hybrid sail. The ± 25.2 deg. lines are the angles of the polar axis of Mars, denoted by dashed lines, with respect to the normal to the orbital plane at the summer and winter solstices respectively. The two quasi-horizontal dashed lines represent the field-of-view exclusion angle of X and Ka-band communications respectively. Points one to four are reference in the text.

Thus, it can be seen that the addition of the sail can reduce the SEP requirements to hover directly above the pole of Mars at the summer solstice, or, equivalently, allow the spacecraft to hover higher than previously possible without the sail. Clearly, in this case it would only make sense to do this over the day-side of the planet, with this region being where the sail is most effective: the volume of space within which equilibria are possible on the night-side of the Earth is severely constrained with a realistic solar sail. This argument is effectively analogous to that made by Ceriotti and M^{c}Innes, who determined families of optimal periodic polesitter orbits above Earth that minimized the SEP propellant consumption over a 1-year period [38], and showed that these optimal orbits are displaced less far out of the orbital plane when on the night-side of Earth.

The enhanced polar opportunities at Mars with hybrid propulsion in turn translate into a partial benefit of using hybrid propulsion for a communications relay at Mars. From Fig. 7, it can be seen that while the hybrid spacecraft can be displaced further from the pole of Mars, it can still only be displaced 0.125AU out of the orbital plane, which is sufficient to complete the relay for the 1.5 degree field-of-view exclusion angle implied by Ka-band communication (represented by the lower quasi-horizontal dashed line in Fig. 7) but not for the 4 degree angle of X-band communication (the dashed upper quasi-horizontal dashed line in Fig. 7). Therefore, considering the region between the two quasi-horizontal dashed lines, on the day-side of Mars, it can be seen there is an area where the addition of a small and technically feasible near-term solar sail to an SEP component has some ability to reduce the thrust required from the SEP component, compared to the pure-SEP equivalent spacecraft. Hence, for the specific case of a Ka-band Earth-Mars communication relay, communicating with an asset on the day-side of Mars in the approximate vicinity of the poles, hybrid propulsion could be an advantage to the mission. However, if the ground assets are located away from the poles then hybrid propulsion proves less advantageous (although this only considers the case of one relay spacecraft, and not two), and if the assets are stationed on the night-side of Mars, then hybrid propulsion provides no advantage. This is also true if the assets are stationed on the day-side during Mars' northern hemisphere winter, since it is important to remember that the poles will rotate, i.e. between northern hemisphere summer and winter the polar axis sweeps out a cone, and hence the benefit of the sail is only felt during the summer.

Utilizing hybrid propulsion in a relay with X-band communication is somewhat more complicated, at least for the case of an artificial equilibrium point located directly above one of the poles, as in Fig. 7. This is essentially due to the second failing of the sail component, namely that of solar flux - in that being so far from the Sun (1.52 AU), the flux of radiation striking the sail and providing the photon pressure is considerably less than that at Earth. The characteristic acceleration of 0.2 mms^{-2}, which is a reasonable near-term goal for solar sail technology, only translates into an actual maximum acceleration of approximately 0.087 mms^{-2} at Mars. This is only a small fraction of the 0.3 mms^{-2} being considered for a 1-tonne SEP spacecraft with 300mN of maximum thrust, and is obviously compounded by the fact that the solar sail acceleration is a function of the sail pitch angle, reducing that value still further as the sail is moved out of the orbital plane. Therefore, it is clear that it will require a significantly advanced solar sail in order to provide sufficient acceleration at Mars to either reasonably reduce the burden on the SEP

thruster to maintain a given AEP, or to hover further above the AEP for a pure SEP spacecraft. Such a scenario is illustrated in Fig. 8, where the hybrid equithrust contours, with the same parameters as before but with a solar sail of characteristic acceleration of 1 mms^{-2}, five times greater than that suggested as realistic in the near-term, are shown. The equivalent thrust contours of the pure SEP system are overlaid in thin black lines and the field-of-view exclusion of X and Ka-band communications is once again represented. Note that the apparently empty region in Fig. 8 at approximately 0.1 AU out-of-plane represents the region where the required SEP thrust is virtually zero, as the solar sail provides all the required thrust.

It can be seen from Fig. 8 how, with this much greater performance hybrid sail, a relay spacecraft could hover at greater distances above Mars if it was displaced closer to or further from the Sun, with it being possible to station up to 0.226 AU above Mars (although not directly) as opposed to 0.176 AU for the pure-SEP system. Equivalently the relay spacecraft could hover at the same distance of 0.176AU out of the orbital plane, except displaced 0.07AU closer to the Sun - with this performance of sail, the SEP thrust needed is just 184mN, as opposed to a pure-SEP system of 300mN. The minimum amount of thrust required from the SEP component with this solar sail to have a Martian polesitter that would be able to complete the relay in X-band communication would be approximately 180mN – this would require approximately 500mN with SEP alone. In this case perhaps the best trade-off would be to have a hybrid with solar sail of characteristic acceleration of 0.6mms^{-2} and SEP maximum thrust of 300mN, which would just allow a polesitter in X-band to complete the relay.

It should be remembered here that the analysis only assumes the case of a large SEP system and small solar sail. However, what is evident is that for this particular combination the hybrid sail is most effective in the orbital plane, where, given the direction of the solar radiation pressure, the sail can be oriented to provide exactly the same component of acceleration $\boldsymbol{a}_{gc}$ as the equivalent performance SEP thruster. This fact may be of greater use in other potential non-Keplerian orbit missions, especially for those closer to the Sun where the photon pressure is higher. One such mission, that of solar storm warning, will be discussed in Section IV.

Power requirements

To actually enable such a mission as the Mars communication relay, the power requirements of the spacecraft must be considered. A simple thruster model, in which the power delivered by the solar arrays is proportional to $1/r_s^2$, where r_s is the distance from the Sun in AU, is applied. A low-thrust ion engine with high specific impulse thus presents a systems engineering issue. This is because, if a standard ion engine with a typical specific power of 27-30 W/mN is considered, the power system would need to deliver between 8 and 9 kW. If a solar array efficiency of 0.25 at 1AU (beginning-of-life) is assumed, with an inherent degradation of 0.8, and a 0.7 reduction due to end-of-life degradation, then 8-9 kW correspond to an area of the solar arrays between 42 and 47 m^2 only for the propulsion system and without margins.

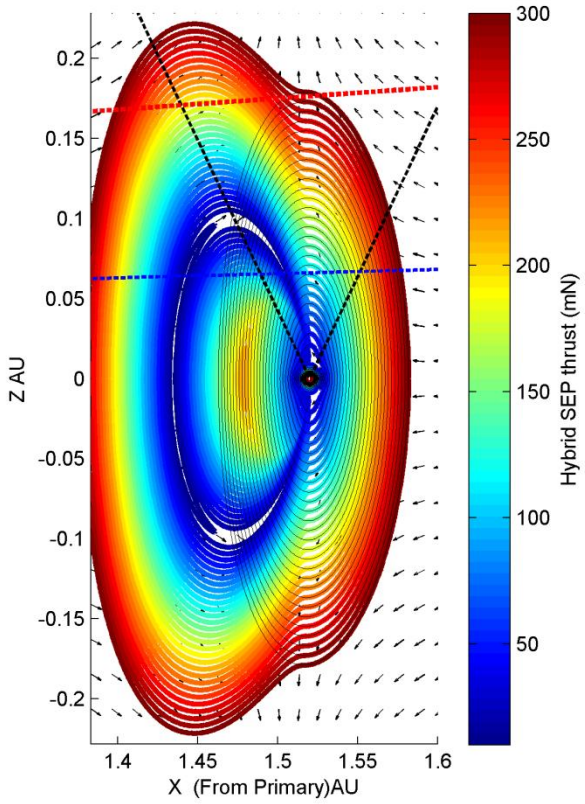

Fig. 8 NKO equithrust contours at Mars, projected onto the plane perpendicular to the orbital plane, for the hybrid solar sail with sail characteristic acceleration 1mm s^{-2}. The thin black contours represent the contours for an equivalent pure-SEP system. The two quasi-horizontal dashed lines represent the field-of-view exclusion angle of X and Ka-band communications respectively.

It is thus required that the thrust level and/or the I_{sp} are substantially lowered, in order to reduce the solar array area to a more attainable value. If one instead assumes a thruster capable of producing a reduced thrust level of 220mN at a distance of 1AU, namely an Astrium RIT-XT engine operating at 3000s with a 22W/mN of specific power, then the required area of the solar arrays would be just 25.3m^2, for the propulsion system only (with no margin, and 25% efficiency of the cells). If a 500W total subsystem power requirement is considered then that area increases to 39.1m^2, if a 20% margin is also included. For comparison, consider the Rosetta and SMART-1 missions – the former had a solar array area of 61.5m^2 for (approximately) a 3000 kg spacecraft [40], and the latter had a solar array area of about 10m^2 for (approximately) a 370 kg spacecraft [41]. Thus the spacecraft for an AEP relay mission at Mars would be somewhere in between Rosetta and SMART-1's requirements.

If the thruster could indeed produce 220mN thrust at 1 AU, that would correspond to 80mN at the aphelion of Mars, which is, as discussed previously, the thrust level required for the Mars relay architecture option featuring two spacecraft each displaced 45 degrees out of the orbital plane and utilising Ka-band radio communication. For details

of how a spacecraft could be inserted into an orbit to enable such a relay, using the values of thrust and specific impulse of the Astrium engine, see [42].

Contingency Analysis

In order to explore possible recovery options, should the spacecraft suffer thruster failure during the mission to enable continuous communications between Earth and Mars, various contingency scenarios were also analyzed using a direct transcription method based on Finite Elements in Time generated on spectral basis [43, 44], while the equinoctial equations of motion in the Gauss' form were used to describe the spacecraft motion [45 ,46]. This was combined with a general consideration of how best to utilize the spacecraft between occultations - since the spacecraft are only required to provide a relay service during occultation, maintaining the AEP for a full synodic period is not necessary, and thus one potential strategy is to let the spacecraft drift away from the AEP in between two occultation periods, to conserve fuel. If no contingency occurs, maneuvers can be planned to re-acquire the AEP at minimum propellant cost after one synodic period.

As discussed previously, the blackout period caused by solar conjunction is on the order of one month. However, for the purposes of building significant robustness into the period of communication during conjunction, given the importance of maintaining contact with a human crew as opposed to a robotic one, it was assumed in this study that the blackout period is order of 3 months (90 days). This would therefore allow for optimal communication between Mars and Earth, without having to worry about potentially compromising data rates by "pinching" the Sun-Earth-Mars angle too significantly (e.g., if the conjunction period is scheduled for 40 days, even if direct communication between Earth and Mars is possible before and after this period, it may be significantly less than optimal, and there is no sense in only having the relay spacecraft in position for 40 days). Of course, in a later study this 90 day period could be significantly reduced and fine-tuned as the exact conjunction period was determined, but it provides a reasonable order of magnitude, including sensible margins, for a first-order consideration.

For the analysis, the maximum thrust level of each spacecraft is assumed to be 80mN and the I_{sp} is 3000s. Both relay spacecraft are initially in the position as discussed previously for a relay using Ka-band communications – that is, an AEP displaced 45 degrees above the orbital plane, using a thrust of 80mN. This corresponds to a distance of approximately 7 million kilometers above the orbital plane, and the same distance ahead or behind of the planet, as shown in Fig. 9. From these points trajectories are designed to transfer the spacecraft, either from the leading artificial equilibrium point to the trailing AEP (or vice-versa), or from an AEP back to the same AEP - with the goal of having the two spacecraft back in position in displaced orbits in time for the next occultation to begin. The trajectories are optimized to use the least amount of propellant.

The case in which no contingency occurs is shown in Fig. 10, i.e. maneuvers are planned to leave the leading (or trailing) point and reach the trailing (or leading) point, one synodic period later. In this case, the two transfers are symmetric.

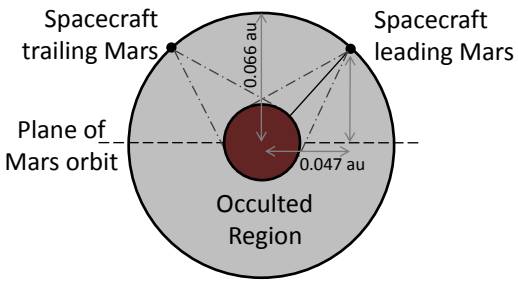

Fig. 9 Initial relative positions of relay spacecraft before transfer for contingency analysis, viewed end-on as from behind Mars.

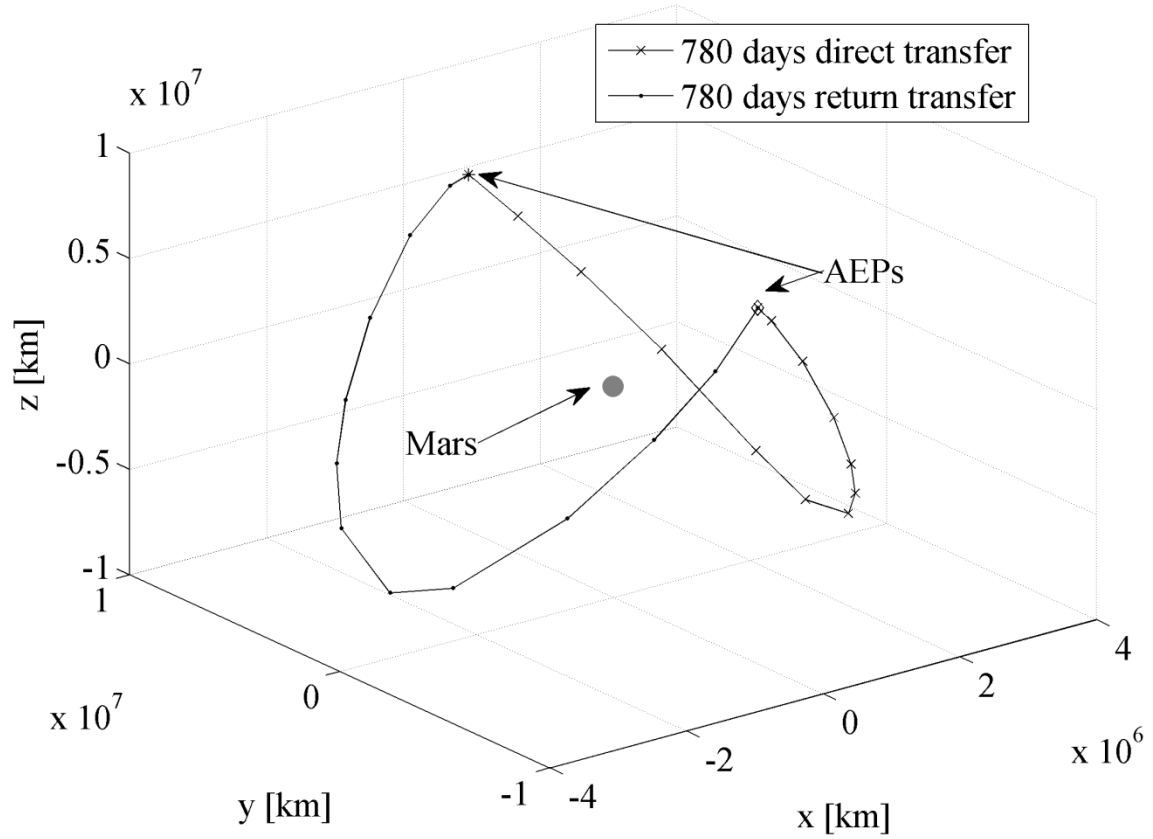

Fig. 10 Transfer of relay spacecraft from one AEP to the other, with no drift.

The case in which the spacecraft is at an AEP and experiences a failure for 340 days is shown in Fig. 11. From either AEP, the spacecraft drifts downwards until the thruster goes back online and a recovery is performed to reach the opposite AEP. Table 2 provides a summary of these the two cases. In the table the forward transfer refers to the leading-to-trailing transfer and the return transfer refers to the trailing-to-leading transfer.

In the case of a failure recovery after 340 days the leading-to-trailing transfer is quite inexpensive. However, the trailing-to-leading transfer has a substantial cost. The total cost for a roundtrip would be about 32.74 kg every 1562.2 days. Note that since, in these calculations, the mass of the spacecraft is assumed to be 1000 kg at the beginning of every transfer, then the total propellant consumption is a slight overestimation of the actual expected cost. Table 2 also shows that, if the maneuvers are planned and no failure occurs (i.e. 0 day drift case), the total cost of a roundtrip reduces to about 14.5 kg every 1562.2 days, or, equivalently, 14.5kg in total across two spacecraft switching position in 781.1 days. Therefore, an exchange of position between trailing and leading points is relatively inexpensive.

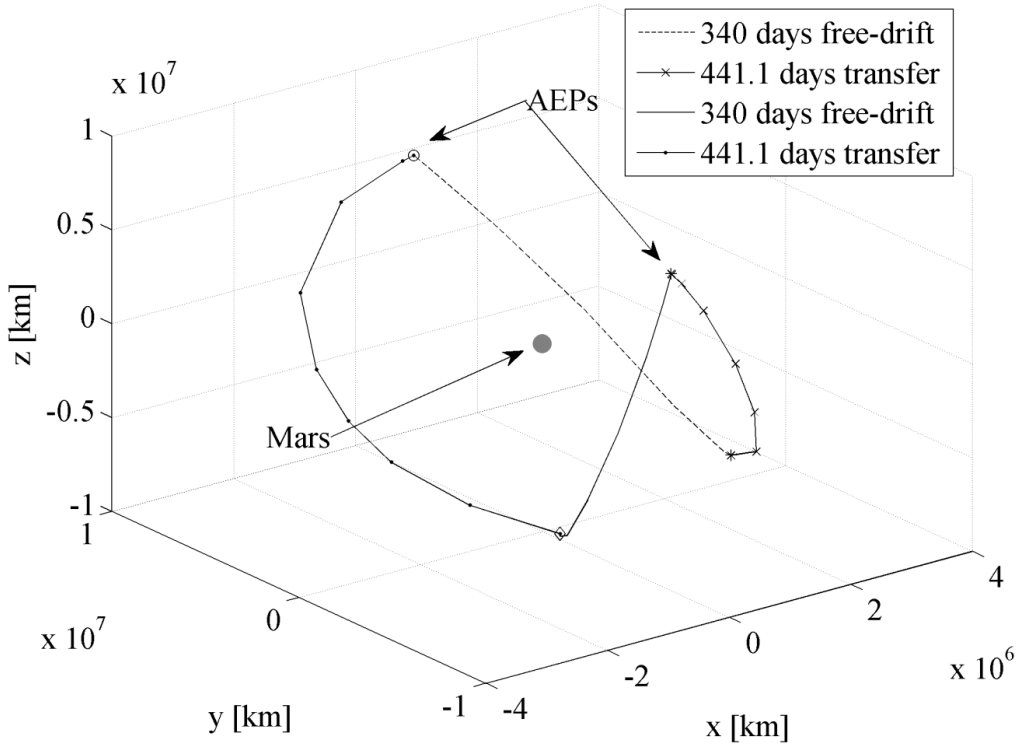

Fig. 11 Recovery transfer from a 340 days drift away from either AEP

Table 2: Summary of leading-to-trailing/trailing-to-leading transfer

	Specific impulse Isp (s)	Total propellant consumed m_p (kg)	m_p (kg) forward transfer	m_p (kg) return transfer	Time of Flight (days)
340 day drift	**3000**	**32.7**	**4.6**	**28.1**	**780+780**
0 day drift	**3000**	**14.5**	**4.6**	**9.9**	**780+780**

An alternative scenario is that the spacecraft is maneuvered to return to the original AEP. Thus, if no contingency occurs, leading-to-leading transfers and trailing-to-trailing transfers are planned to re-acquire respectively the leading and the trailing AEP. If a failure occurs, the spacecraft drifts away and after a number of days the recovery maneuver starts. The cost of a recovery maneuver is evaluated for a drift time of 0, 100, 200, 300 and 390 days. The propellant cost is represented in Fig. 12, where the drift time is called time-to-intervention, and the resultant analysis shows that if no failure occurs, an AEP-to-AEP transfer has a minimal cost of less than 8 kg, for the roundtrip, for the leading point and less than 5 kg roundtrip for the trailing point.

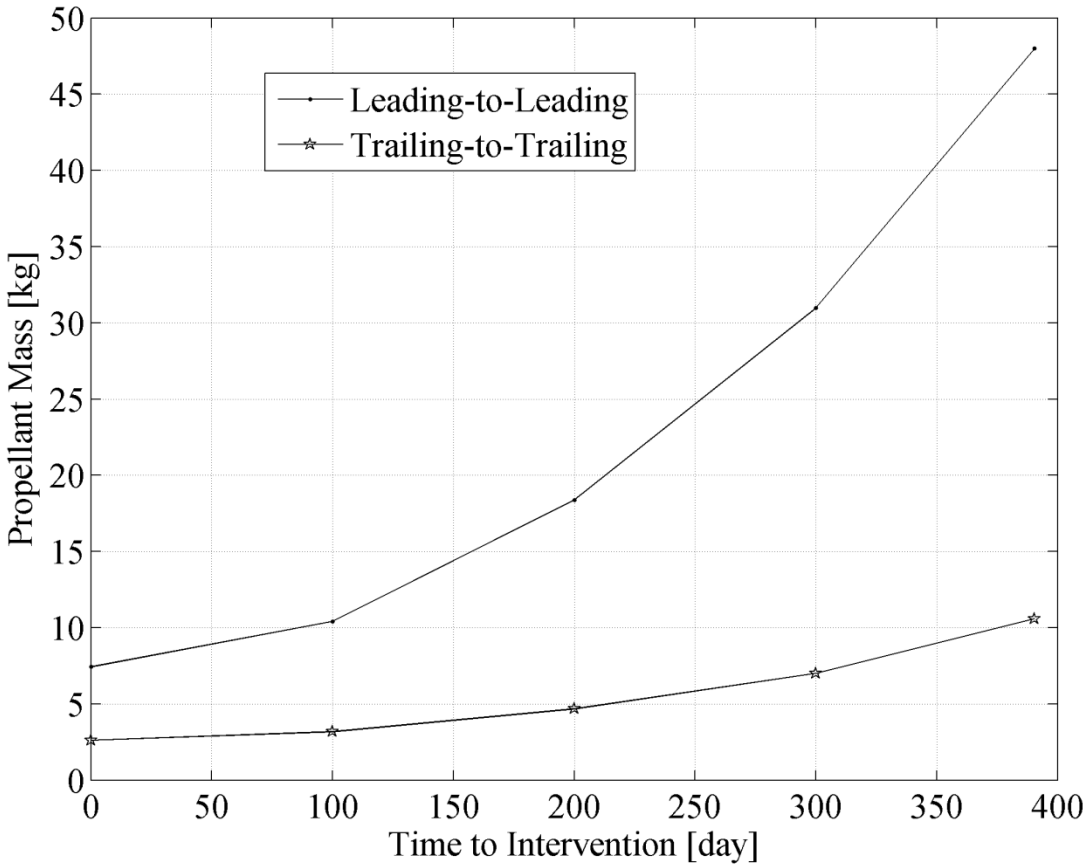

Fig. 12 Propellant cost against time-to-intervention for AEP-AEP contingency transfer

In the case of a failure at the leading point, the cost can grow up to 50 kg roundtrip while it remains contained for a failure at the trailing point. In the former case the spacecraft flies around Mars before re-acquiring the AEP, in the case of a drift time of 390 days. Therefore, if a single spacecraft is used and a failure occurs at the leading point a leading-to-trailing transfer is recommended. Vice versa, if a contingency occurs at the trailing point a trailing-to-trailing transfer is recommended.

This analysis optimizes the return to the AEP to minimize the propellant consumption. However, the return time (time to go from one AEP back to the same AEP), in some cases, could be 681 days, i.e. 100 days before the next occultation. This situation is unfavorable because the spacecraft would need to maintain the AEP with constant thrust for an extra 100 days every synodic period, in addition to the 90 day-burn already planned for during the occultation. An approximate estimate suggests thrusting at the AEP for the extra 100 days would require around 23kg of propellant, in addition to the less than 8 or 5 kg required to do this fuel-efficient transfer, resulting in total propellant consumptions of 31kg and 28kg (approximately).

Instead, the spacecraft can be forced to return to the AEP after 1 synodic period exactly, as shown in Fig. 13, which shows the transfer trajectories for different drift times, while Fig. 14 shows the propellant consumption for different drift times. From Fig. 14, it can be seen that for the trailing AEP the cost remains almost constant (the variation is between 24 and 25 kg) for different drift times.

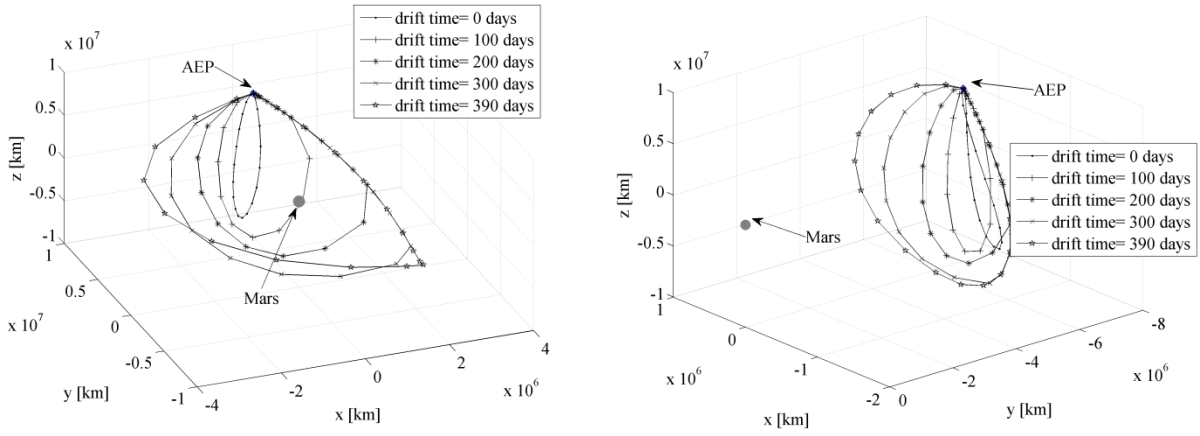

Fig. 13 Families of AEP-AEP contingency transfers with fixed return period; leading-to-leading, left, trailing-to-trailing, right.

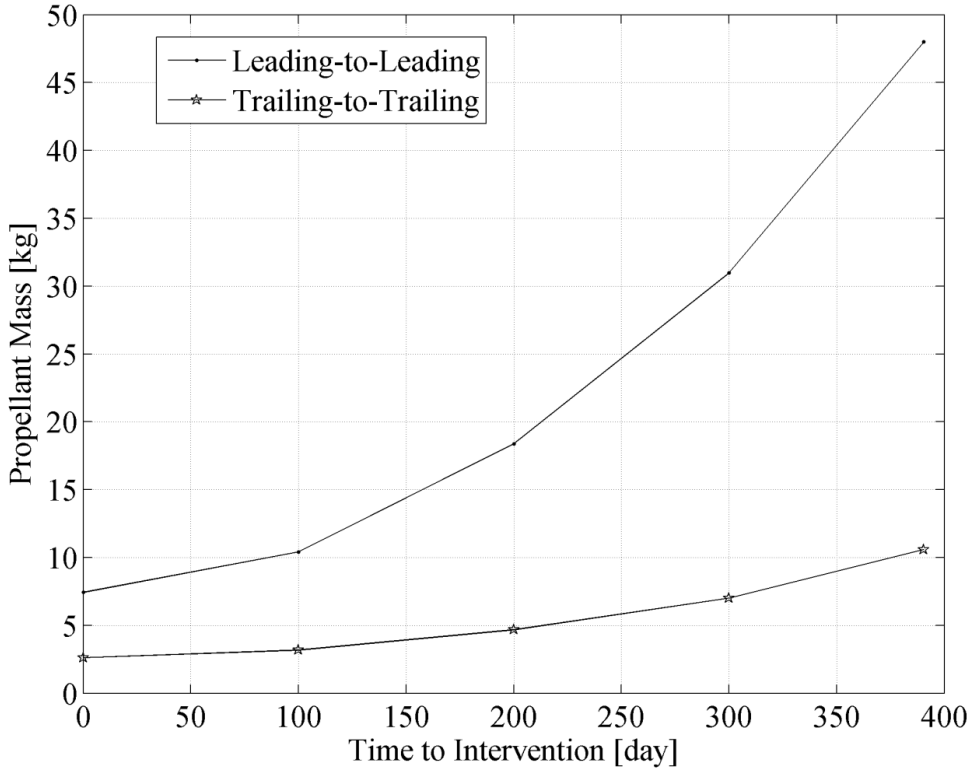

Fig. 14 Propellant cost against time-to-intervention for AEP-AEP contingency transfer. Fixed return period.

Fixing the leading-to-leading or trailing-to-trailing re-acquire time to 1 synodic period results in propellant consumptions of 25 and 24 kg, approximately, which is clearly more efficient overall than the previous situation where the transfer trajectory itself is optimized for fuel efficiency but the spacecraft comes back to the AEP too early and has to expend a lot of energy to stay there. However it must be noted that this is still less efficient than the AEP-swapping system, which requires a total of around 14.5kg for two spacecraft to switch position from leading-to-trailing and vice-versa in one synodic period. Again, if the engine fails to thrust, the situation can be recovered with increasing amounts of propellant for ever-increasing failure times, although interestingly only for the leading-to-leading case (where the increase is dramatic, as per before), with it being approximately constant for the trailing-to-trailing case.

Of course, it is worth pointing out that all the propellant consumption figures have the potential to be significantly reduced by determining the exact length of time the conjunction will disrupt communications for once the mission profile is determined, and then tuning the relay spacecraft to occupy an AEP for this length of time. The amount of propellant required to transfer the spacecraft may not change a great deal, as optimal trajectories can be designed to take into account the longer transfer time, but the amount of propellant required to occupy the AEP will decrease significantly as the time it has to be occupied for decreases.

Finally, it is worth remembering that, in-between periods of occultation when the AEP is no longer need to be maintained by the relay spacecraft, there are already existing communications relays which provide virtually continuous coverage of the entire Martian surface - as outlined by e.g. Strizzi et al. [32] and Pernicka, Henry & Chan [47]. Thus, it is envisaged that continuous communications for the entire synodic period of a Martian orbit would be achieved by both the mechanism outlined in these aforementioned references and the one discussed at length in this paper. This could be done either by having four spacecraft, two at the Lagrange points in halo orbits and two to occupy the artificial equilibrium points when required, or by investigating the possibility of only having two relay spacecraft and transferring them into the alternating halo/non-Keplerian orbits as required.

Extension to elliptic restricted three-body problem

In detailing such a communications relay, non-Keplerian orbits formulated in the circular restricted three-body problem (CRTBP) were considered for simplicity. However, the implications of eccentricity (of the primaries) on the required instantaneous thrust and Δv are considered here by recasting the problem into rotating-pulsating coordinates associated with the elliptic restricted three-body problem (ERTBP).

When the effect of eccentricity is included, the continuous low-thrust required to induce a displaced periodic orbit in the inertial frame that corresponds to an artificial equilibrium point in the rotating-pulsating frame is no longer constant, but varies with true anomaly over an orbit – with the acceleration in the ERTBP required to occupy an equilibrium point in the rotating-pulsating frame being given by a low-thrust feed-forward control of the form,

$$\begin{aligned} u_x &= a_x(1 + e\cos f)^2 \\ u_y &= a_y(1 + e\cos f)^2 \\ u_z &= (a_z + ze\cos f)\,(1 + e\cos f)^2 \end{aligned} \tag{11}$$

where a_x, a_y, and a_z are constant, e is the eccentricity of the orbit, and f is the true anomaly. Note that the accelerations are given in non-dimensional units– for the full details of this derivation, see Appendix A. Note also that when *e=0* the controls degenerate to the constant thrust required to induce non-Keplerian orbits in the CRTBP.

It should firstly be stated that the CRTBP provides a good approximation, because in the ERTBP, over the course of an orbit, the time-average of the behavior is approximately equivalent - even for relatively extreme examples of eccentricity such as Mercury (e = 0.21). Moreover, it is shown that the effect of the eccentricity on the Δv per orbit of the spacecraft is negligible. However, the instantaneous value of the thrust required to occupy approximately the same point during an orbit can be significantly different. This effect must be quantified for the Earth-Mars relay to demonstrate the practicalities of implementing such a mission.

For example, consider the case of the relay with a single pure-SEP spacecraft, which requires 300mN of thrust to displace high enough above Mars to enable a relay in X-band communications in the CRTBP. In this case the thrust would be constant but in the ERTBP it would need to smoothly vary according to Eqs. (11), as shown in Fig. 15.

In this example the minimum instantaneous value of thrust required to occupy this point would be 225mN, and the maximum value would be 392mN. Over the course of an orbit the average value of the thrust is approximately 302mN, which is only 0.7% greater than the constant thrust requirement in the CRTBP. However, when considering the feasibility of a mission involving non-Keplerian orbits, the eccentricity of the primary bodies will have a significant impact on the catalogue of orbits obtainable given a maximum instantaneous thrust capability.

This slight increase in the average thrust per orbit required in the ERTBP to occupy approximately the same point of that of the CRTBP leads to an increase in the required Δv per orbit. An indefinite integral for the Δv, given the feed-forward control acceleration in Eqs. (11) is given by,

$$\Delta v = \int \sqrt{\left(a_x^2 + a_y^2 + (a_z + ze\cos f)^2\right)(1 + e\cos f)^4}\, df \tag{12}$$

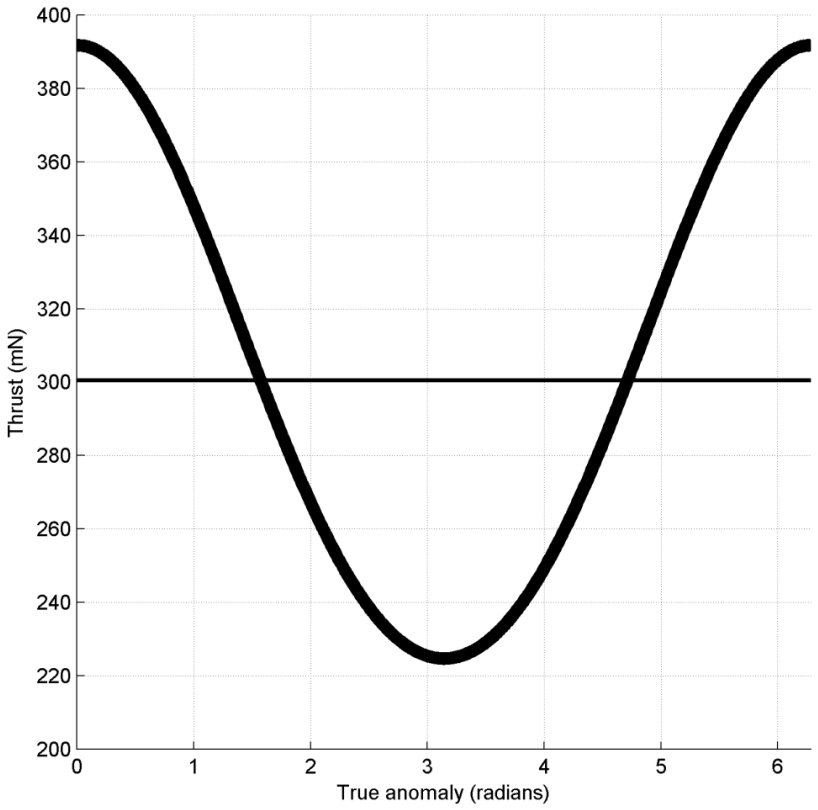

Fig. 15 Variation of required thrust with true anomaly for a contour in the x-z plane in the Sun-Mars ERTBP ($e = 0.09$-thick line) that could be occupied with a thrust of 300mN in the CRTBP (e=0-thin line).

A useful analytic approximation of this can be derived by expanding the integrand to 3rd order in e about $e = 0$ and integrating with respect to the true anomaly over one orbit period $0 \leq f \leq 2\pi$. Defining the constant $K = a_x^2 + a_y^2 + a_z^2$ for simplicity the approximate Δv per elliptic non-Keplerian orbit, call Δv_e, is,

$$\Delta v_e = \frac{\pi(2K^2\,(2+e^2) + 4a_z K e^2 z + \left(a_x^2 + a_y^2\right)e^2 z^2)}{2K^{3/2}} \tag{13}$$

Note that when $e = 0$ the Δv per orbit reduces to $\Delta v_0 = 2\pi\sqrt{a_x^2 + a_y^2 + a_z^2}$, corresponding to the non-dimensional constant thrust magnitude in the circular case. The percentage increase in Δv per orbit due to eccentricity is then given by $100 \times (\Delta v_e - \Delta v_0)/\Delta v_0$, which is explicitly,

$$\%\, change\ in\ \Delta v = 25e^2(2 + \frac{z\left(4a_z K + z\left(a_x^2 + a_y^2\right)\right)}{K^2}) \tag{14}$$

This calculation gives an indication of how the eccentricity will affect the Δv requirement for non-Keplerian orbits. For example a 1000 kg spacecraft in a displaced non-Keplerian orbit at x = 1.5451 AU from the Sun, y = 0.0838 AU and z = 0.0419 AU from Mars, where x, y, z are rotating-pulsating co-ordinates requiring continuous constant acceleration in the circular case of $a_x = 1.3881 \times 10^{-4} ms^{-2}, a_y = 7.3153 \times 10^{-6} ms^{-2}, a_z = 6.7045 \times 10^{-5} ms^{-2}$ (converting into non-dimensional units and substituting into (14)) gives a percentage change in Δv per orbit due to eccentricity ($e = 0.09$) of 0.6%. As such, while the effect of eccentricity cannot be neglected when considering the instantaneous thrust requirements, the time averaged effect of eccentricity on Δv can be neglected in this first-order analysis.

IV. A Hybrid Propulsion Solar Storm Warning Mission – AreoStorm

Currently, probes at the Earth-Sun L_1 point can provide approximately 30 minutes advance warning of an approaching Coronal Mass Ejections (CME). In 1999, the ST-5 GeoStorm mission proposal suggested the use a solar sail of characteristic acceleration 0.169mm s^{-2} to access an artificial displaced orbit at a point sunward of Earth-Sun L_1 point (0.993AU from the Sun), maintaining station at 0.985 AU [10]. Such a spacecraft would increase the warning time of an approaching magnetic storm by a factor of approximately 3. For future human or enhanced robotic exploration of Mars knowledge of approaching solar storm will be even more critical than at Earth, as the thinner Martian atmosphere and weaker magnetic field will provide significantly less natural protection, and a human crew may be some distance from suitable shelter. However, due to the inverse square reduction in solar sail acceleration with distance from the Sun, the ST-5 sail would provide an acceleration of only 0.07 mm s^{-2} at Mars. Such a sail would in-turn enable a 100 kg spacecraft in an artificial displaced orbit at a point sunward of Mars-Sun L_1 point (1.513AU from the Sun), maintaining station at 1.506 AU from the Sun, in-effect doubling the warning time of a spacecraft in a Mars L_1 halo orbit.

A similar mission concept can be considered with a continuous low-thrust SEP spacecraft. Assuming once again, a spacecraft mass of $m = 1000$kg, with a thrust magnitude of 80 mN, as discussed previously, an AEP can be enabled at a distance of approximately 1.503 AU from the Sun, increasing the storm warning time over a spacecraft in a Mars L_1 halo orbit by a factor of 2.5. Consider now the addition of a solar sail to such an SEP mission concept. Using the same parameters as those in Fig. 7, that is, a solar sail of characteristic acceleration 0.2 mm s^{-2}, it can be seen that this warning time can be further improved, as illustrated by Fig. 16, due to the additional acceleration contribution made by the solar sail. Note that this slightly higher characteristic acceleration, than the ST-5 sail, would in-effect provide a matching pure solar sail performance, with a total mass again of 100 kg, to the previously discussed pure SEP mission.

Once again limiting the SEP thrust magnitude to 80 mN, it is seen from Fig. 16 that an AEP can be enabled at a distance of approximately 1.485 AU from the Sun, increasing the storm warning time over a spacecraft in a Mars L_1 halo orbit by a factor of five, assuming a CME has a constant propagation speed, which is not strictly true, but is a reasonable assumption for this analysis. Equivalently, the solar sail can be used to reduce the required thrust magnitude from the SEP system, at the expense of storm warning time, and hence extend the spacecraft operational lifetime.

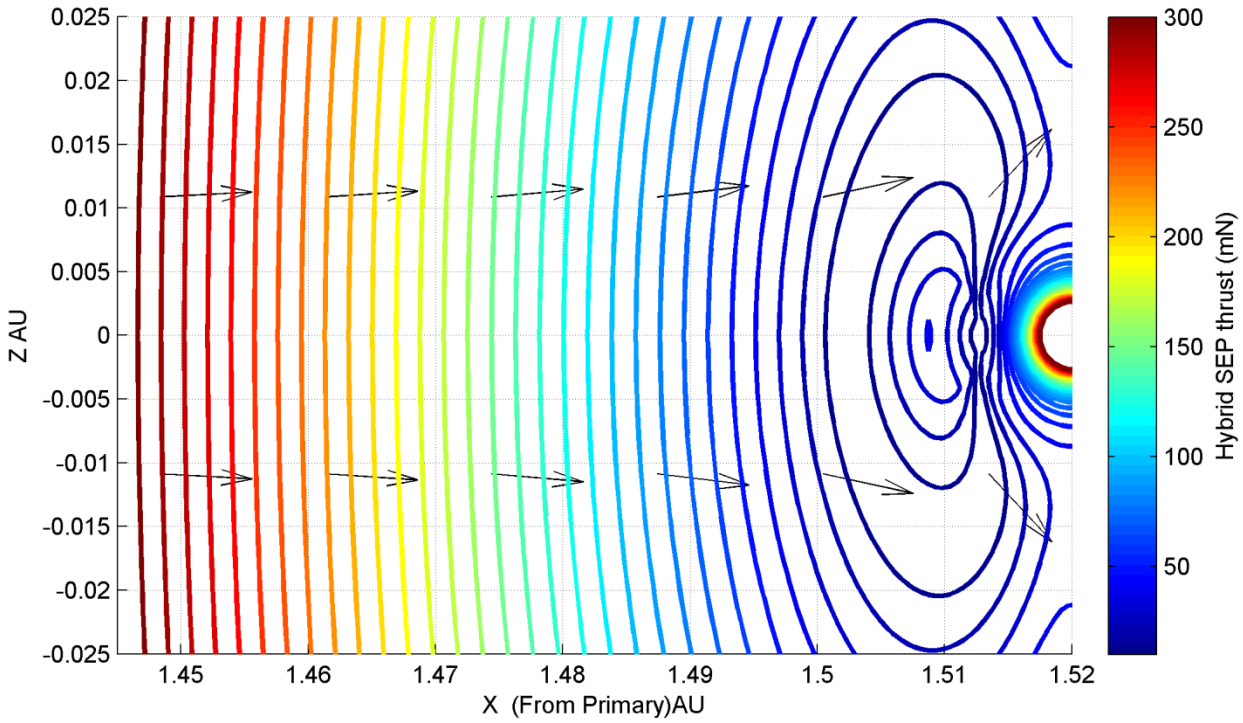

Fig. 16 NKO equithrust contours, with thrust direction arrows, at Mars, projected onto the plane perpendicular to the orbital plane, for a hybrid sail with characteristic acceleration 0.2 mm s^{-2} and other parameters as given in the text.

It is also of interest to push the design parameters of such a hybrid spacecraft and determine what thrust and/or solar sail would be needed to achieve a warning time increase of a factor of about 10 over that given by stationing at L_1. Such a warning spacecraft must be stationed at approximately 0.07 AU from Mars and would require a total thrust magnitude of order 290 mN. Table 3 summarizes how a hybrid spacecraft can trade-off the available SEP thrust magnitude, ranging from 80 – 145 mN, with the sail characteristic acceleration, ranging from 0.3 – 0.5 mm s^{-2}, to achieve a factor of 10 increase in storm warning time. Table 3 also summarizes the previous results of this section, which are then also detailed in Fig. 17 which shows the corresponding the sail design space for each mission detailed in Table 3. In Fig. 17 the sail area is determined from the payload fraction the sail is able to carry given a non-sail mass of 1000kg for a given characteristic acceleration, assuming a range of sail assembly loading values.

It can be seen from Fig. 17 that the available design space decreases as the sail performance increases. But from Table 3 and Fig. 17 together it can be seen that in future it may be possible to trade-off development of one aspect of the hybrid against the other, depending on mission requirements. Solar Electric Propulsion is the more mature technology, in relative terms at least, and so improvements in that technology may be more incremental and reliable in the short term, but the potential of solar sailing is almost completely untapped, being as it is considerably less well-developed. Additionally, one of the major benefits of increasing sail performance is to help to reduce the propellant consumption from the SEP part, and thus extend mission durations significantly.

Table 3: Summary of potential AreoStrorm missions

Opportunity Name	**Approximate station distance from Mars (AU)**	**SEP Thrust (mN)**	**Sail acceleration**		**Magnitude of storm warning time factor**
			Characteristic (mm s^{-2})	**Actual (mm s^{-2})**	
L_1 station	0.007	0	0	0	1
Pure Sail (ST-5)	0.014	0	0.17	0.074	2
Enhanced Pure Sail	0.018	0	0.20	0.087	2.57
Pure SEP	0.017	80	0	0	2.43
Hybrid, as per Fig. 16	0.035	80	0.20	0.087	5
x10 Warning, a	0.070	80	0.49	0.210	10
x10 Warning, b	0.070	100	0.44	0.190	10
x10 Warning, c	0.070	120	0.393	0.170	10
x10 Warning, d	0.070	145	0.335	0.145	10

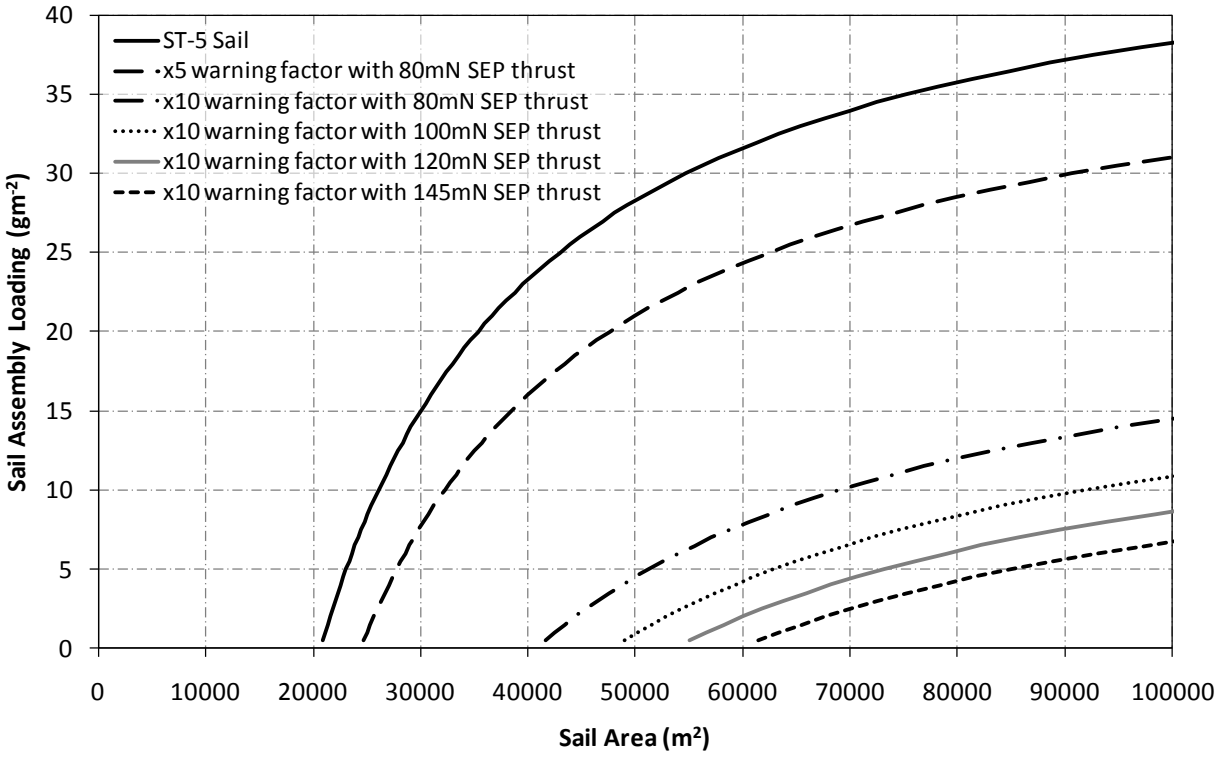

Fig. 17 Solar sail design space for the hybrid AreoStorm mission with varying warning storm.

Of course, it is important to remember here that although equithrust surfaces are considered, no propulsion system actually delivers an equal thrust throughout the lifetime of the spacecraft, due to either depletion of reaction-mass or, in the case of solar sailing, the degradation of the optical surface [33]. As such, the propulsion system would have to be throttled to adjust for either the increasing (for depletion of reaction-mass) or decreasing (for degradation of the optical surface) acceleration vector magnitude. It is also worth commenting that this is not a true like-for-like comparison, in terms of the mass of the pure-SEP and hybrid spacecraft. The above discussion simply compares the acceleration available to two different spacecraft, and thus, in that respect, it is reasonably obvious to say that adding a sail to an SEP system will produce better performance than a pure-SEP system alone - but it is still useful to quantify exactly how much better, given achievable solar sail performances. A more in-depth analysis (beyond the scope of this paper) would require a detailed mass budget for both spacecraft to be determined and from that the relative acceleration of a pure-SEP spacecraft and a hybrid spacecraft of equal masses could then be compared.

V. Conclusion

Two novel mission concepts have been presented which use continuous and constant low-thrust propulsion to enable highly non-Keplerian orbits in support of future high-value asset exploration of Mars. Detailed analysis of a Mars communications relay showed that current, or near-term, technology, such as the QinetiQ T6 thruster can be used to enable continuous communications between Earth and Mars during solar conjunctions, it was also found that a Ka-band communication system, rather than an X-band system, significantly relaxed the propulsion system requirements. The use of solar electric propulsion and a hybrid solar sail/solar electric propulsion spacecraft were considered for the communication relay, the addition of a modest solar sail proves some advantages for the case of a communications relay using Ka-band and particularly for communication with assets stationed near the poles during summertime. Several propulsion system failure and contingency schemes were considered, with it being shown that transferring a spacecraft between potential relay locations is relatively inexpensive. Analysis of a solar storm warning mission was presented for the first time. It was found that for this mission to provide a meaningful advantage over a conventional Sun-Mars L_1 halo orbit a hybrid solar sail/solar electric propulsion spacecraft was required. Such hybrid propulsion was found to reasonably offer a factor of five increase in warning time. Finally, the effect of Mars orbit eccentricity was briefly considered and found to impact the time averaged analysis, however the effect of Mars orbit eccentricity was found to be significant when considering maximum and minimum instantaneous force requirements.

Appendix A: Derivation of the feed-forward control accelerations in the ERTBP

The elliptical restricted three-body problem (ERTBP) including continuous low-thrust propulsion in the rotating-pulsating frame can be used as the dynamical model to describe a low-thrust spacecraft under the gravitational influence of two massive bodies. This model is derived by performing a simple coordinate change from the rotating-barycentric frame to the rotating-pulsating frame. In order to obtain the equations of motion in the most convenient form the equations are derived using the procedure of Gurfil and Meltzer [48].

The small primary orbits the large primary on an elliptic orbit with eccentricity e, which complies with the two-body Keplerian motion. The distance between the two primaries, ρ, depends upon the true anomaly, f, through the conic equation,

$$\rho = p/(1 + e\cos f) \qquad (A1)$$

where p is the semi-latus rectum $p = a(1 - e^2)$ and a is the semi-major axis. The rate of change of the true anomaly satisfies $\dot{f} = h/\rho^2$ where h is the magnitude of the angular momentum, given by $h^2 = G(m_1 + m_2)p$. Here G is the universal gravitational constant and m_1, m_2 denote the mass of the first and second primary respectively. An appropriate set of units is introduced so that the gravitational constant $G = 1$, the semi-major axis $a = 1$ and we define the constant $\mu = m_2/(m_1 + m_2)$ where m_1 is located at $[-\rho\mu, 0,0]^T$ and m_2 is located at

$[\rho(1-\mu),0,0]^T$. The position vector of the spacecraft in the rotating barycentric frame is given by $\boldsymbol{R} = [X, Y, Z]^T$. The coordinate system rotates at a rate $\dot{f}$ about the z axis so that the angular velocity vector is $\boldsymbol{\omega} = \left[0,0,\dot{f}\right]^T$ and the velocity vector $\boldsymbol{V}$ is:

$$V = \dot{\boldsymbol{R}} + \boldsymbol{\omega} \times \boldsymbol{R} = \left[\dot{X} - \dot{f}Y, \dot{Y} + \dot{f}X, \dot{Z}\right]^T \tag{A2}$$

The position of the low-thrust spacecraft with respect to the primaries is then expressed as $\hat{\boldsymbol{r}}_1 = [X + \mu\rho, Y, Z]^T$ and $\hat{\boldsymbol{r}}_2 = [X + (\mu-1)\rho, Y, Z]^T$. Denoting the kinetic energy K, the potential energy by U, and the Lagrangian by L, we have:

$$K = \frac{1}{2}V \cdot V, \quad U = -\frac{(1-\mu)}{\|\hat{\boldsymbol{r}}_1\|} - \frac{\mu}{\|\hat{\boldsymbol{r}}_2\|}, \quad L = K - U \tag{A3}$$

Writing the Euler-Lagrange equations with the components of the position vector as the generalized coordinates with the low-thrust propulsion vector $\boldsymbol{u} = \left[u_x, u_y, u_z\right]^T$ gives:

$$\frac{d}{dt}\left(\frac{\partial L}{\partial \dot{\boldsymbol{R}}}\right) - \left(\frac{\partial L}{\partial \boldsymbol{R}}\right) = \boldsymbol{u} \tag{A4}$$

In coordinate form this yields the equations of motion for the low-thrust ERTBP in the rotating barycentric frame of reference:

$$\begin{aligned}
\ddot{X} - \dot{f}^2X - 2\dot{f}\dot{Y} - \ddot{f}Y &= -\frac{(1-\mu)(X+\rho\mu)}{[(X+\mu\rho)^2 + Y^2 + Z^2]^{3/2}} - \frac{\mu[X+(\mu-1)\rho]}{[(X+(\mu-1)\rho)^2 + Y^2 + Z^2]^{3/2}} + u_x \\
\ddot{Y} - \dot{f}^2Y + 2\dot{f}\dot{X} + \ddot{f}X &= -\frac{(1-\mu)Y}{[(X+\mu\rho)^2 + Y^2 + Z^2]^{3/2}} - \frac{\mu Y}{[(X+(\mu-1)\rho)^2 + Y^2 + Z^2]^{3/2}} + u_y \\
\ddot{Z} &= -\frac{(1-\mu)Z}{[(X+\mu\rho)^2 + Y^2 + Z^2]^{3/2}} - \frac{\mu Z}{[(X+(\mu-1)\rho)^2 + Y^2 + Z^2]^{3/2}} + u_z
\end{aligned} \tag{A5}$$

The thrust is included before the coordinate transformation to the rotating-pulsating frame so that a direct comparison can be made with the circular case [24, 42]. To simplify equations (A5) a transformation to the rotating-pulsating coordinates is used [48]. Defining $X = \rho x$, $Y = \rho y$ and $Z = \rho z$ and then transforming time derivatives into derivatives with respect to true anomaly [48] yields:

$$\begin{aligned}
x'' - 2y' &= \frac{\partial \omega}{\partial x} + \frac{u_x}{(1+e\cos f)^3} \\
y'' + 2x' &= \frac{\partial \omega}{\partial y} + \frac{u_y}{(1+e\cos f)^3} \\
z'' &= \frac{\partial \omega}{\partial z} + \frac{u_z}{(1+e\cos f)^3}
\end{aligned} \tag{A6}$$

where $x^{'}, y^{'}, z^{'}$ denote differentiation with respect to the true anomaly, and where the pseudo-potential is given by:

$$\omega = \frac{1}{1+e\cos f}\left(\frac{1}{2}(x^2+y^2-z^2 ecosf) + \frac{1-\mu}{\|\boldsymbol{r}_1\|} + \frac{\mu}{\|\boldsymbol{r}_2\|}\right) \tag{A7}$$

with $\boldsymbol{r}_1 = [x+\mu, y, z]^T$ and $\boldsymbol{r}_2 = [x+(\mu-1), y, z]^T$.

In the rotating pulsating coordinate system displaced equilibrium points correspond to displaced elliptic periodic orbits in the inertial frame. Thus, displaced periodic orbits can be identified by setting $x^{'} = y^{'} = z^{'} = x^{''} = y^{''} = z^{''} = 0$ in Equation (A6), which yields:

$$\begin{aligned}
\frac{\partial \omega}{\partial x} &= -\frac{u_x}{(1+e\cos f)^3} \\
\frac{\partial \omega}{\partial y} &= -\frac{u_y}{(1+e\,cos\, f)^3} \\
\frac{\partial \omega}{\partial z} &= -\frac{u_z}{(1+e\cos f)^3}
\end{aligned} \tag{A8}$$

From Eq. (A8) it can be seen that equithrust contours of equilibrium points do not exist in the ERTBP. However, equilibrium points which correspond to periodic orbits in the inertial frame can be induced by a low-thrust feed-forward control of the form:

$$\begin{aligned}
u_x &= a_x(1+e\cos f)^2 \\
u_y &= a_y(1+e\cos f)^2 \\
u_z &= (a_z + ze\cos f)\,(1+e\cos f)^2
\end{aligned} \tag{A9}$$

where, a_x, a_y, a_z are constant. Substituting (A9) into (A8) then gives the nested surfaces of equilibrium points:

$$\begin{aligned}
a_x &= -x + \frac{\mu(x+\mu-1)}{((x+\mu-1)^2+y^2+z^2)^{3/2}} - \frac{(\mu-1)(x+\mu)}{((x+\mu)^2+y^2+z^2)^{3/2}} \\
a_y &= -y + \frac{\mu y}{((x+\mu-1)^2+y^2+z^2)^{3/2}} - \frac{(\mu-1)y}{((x+\mu)^2+y^2+z^2)^{3/2}} \\
a_z &= \frac{\mu z}{((x+\mu-1)^2+y^2+z^2)^{3/2}} - \frac{(\mu-1)z}{((x+\mu)^2+y^2+z^2)^{3/2}}
\end{aligned} \tag{A10}$$

Since these equations are non-dimensional, to use them in Sections III they must be re-dimensionalized - multiplying by GM/R^2 (where G is the gravitational constant in units of $m^3\ kg^{-1}\ s^{-2}$, $M = M_1 + M_2$ is the mass of the two primaries in kilograms, and R is the distance between the two massive bodies in metres) will transform the accelerations back into physical units of meters per second per second (ms^{-2}).

Acknowledgments

This work was part-funded by ESA Contract Number 22349/09/F/MOS; Study on Gravity Gradient Compensation Using Low Thrust High Isp Motors and by European Research Council Advanced Investigator Grant VISIONSPACE 227571 for C. M^{c}Innes.

References

[1] Dusek, H. M., "Motion in the Vicinity of Libration Points of a Generalized Restricted Three-Body Model", Methods in Astrodynamics and Celestial Mechanics: Progress in Astronautics and Aeronautics, Vol. 17, pp. 37-54, 1966.
[2] McKay, R. J., Macdonald, M., Biggs, J., McInnes, C., "Survey of Highly Non-Keplerian Orbits With Low-Thrust Propulsion", Journal of Guidance Control and Dynamics, In Press, 2011.
[3] Driver, J. M., "Analysis of an Arctic Polesitter", Journal of Spacecraft and Rockets, Vol. 17, No. 3, pp. 263-269, 1980.
[4] Forward, R. L., "Light Levitated Geostationary Cylindrical Orbits", Journal of the Astronautical Sciences, Vol. 29, No. 1, pp. 73-80, 1981.
[5] Forward, R. L., "Light Levitated Geostationary Cylindrical Orbits Using Perforated Light Sails", Journal of the Astronautical Sciences, Vol. 32, No. 2, pp. 221-226, 1984.
[6] Farquhar, R., "Limit Cycle Analysis of a Controlled Libration-Point Satellite", The Journal of the Astronautical Sciences XVII, Vol. 17, No. 5, pp. 267-291, 1970.
[7] Baig, S., McInnes, C.R., "Light levitated geostationary cylindrical orbits are feasible", Journal of Guidance, Control, and Dynamics , Vol. 33, No. 3., pp. 782-793., 2010.
[8] McInnes, C. R., Solar Sailing: Technology, Dynamics and Mission Applications, Praxis Publishing, Chichester, ISBN 1-85233-102-X, 1999.
[9] West, J. L., "The GeoStorm Warning Mission: Enhanced Opportunities Based On New Technology", 14th AAS/AIAA Spaceflight Mechanics Conference, Paper AAS 04-102, Maui, Hawaii, Feb 8-12, 2004.
[10] West, J. L., "Solar Sail Vehicle System Design for the GeoStorm Warning Mission", Structures, Structural Dynamics and Materials Conference, Atlanta, April 2000.
[11] McInnes, C. R., "The Existence and Stability of Families of Displaced Two-Body Orbits," Celestial Mechanics and Dynamical Astronomy, Vol. 67, No. 2, 167-180, 1997.
[12] McInnes, C. R., "Dynamics, Stability, and Control of Displaced Non-Keplerian Orbits," Journal of Guidance, Control and Dynamics, Vol. 21, No. 5, pp. 799-805, 1998.
[13] Morimoto, M. Y., Yamakawa, H., and Uesugi, K., "Artificial Equilibrium Points in the Low-Thrust Restricted Three-Body Problem", Journal of Guidance, Control, and Dynamics, Vol. 30, No. 5, pp. 1563-1567, 2007.
[14] Morimoto, M. Y., Yamakawa, H., and Uesugi, K, "Periodic Orbits with Low-Thrust Propulsion in the Restricted Three-Body Problem", Journal of Guidance, Control, and Dynamics, Vol. 29, No. 5, pp. 1131-1139, 2006.
[15] Spilker, T. R., "Saturn Ring Observer", Acta Astronautica, Vol. 52, pp. 259-265, 2003.
[16] Sawai, S., Scheeres, D. J., and Broschart, S., "Control of Hovering Spacecraft using Altimetry", Journal of Guidance, Control, and Dynamics, Vol. 25, No. 4, pp. 786-795, 2002.
[17] Broschart, S. B., and Sheeres, D. J., "Control of Hovering Spacecraft Near Small Bodies: Application to Asteroid 25143 Itokawa", Journal of Guidance, Control, and Dynamics, Vol. 28, No. 2, pp. 343-354, 2005.
[18] McInnes, C. R., "Dynamics, Stability and Control of Displaced Non-Keplerian Orbits", Journal of Guidance, Control, and Dynamics, Vol. 21, No. 5, September-October 1998.
[19] Macdonald M., McInnes, C. R. "GeoSail; An Enhanced Magnetosphere Mission, Using a Small Low Cost Solar Sail", Proceedings of 51st International Astronautical Congress, IAC Paper 00.W.1.06, Rio de Janeiro, Brasil, Oct 2-6, 2000.
[20] McInnes, C. R., Macdonald, M., Angelopolous, V., and Alexander, D., "GEOSAIL: Exploring the Geomagnetic Tail Using a Small Solar Sail", Journal of Spacecraft and Rockets, Vol. 38, No. 4, pp. 622-629, 2001.

[21] Macdonald, M., Hughes, G.W., McInnes, C. R., Lyngvi, A., Falkner, P., Atzei, A., "GeoSail: An Elegant Solar Sail Demonstration Mission", Journal of Spacecraft and Rockets, Vol. 44, No 4, pp. 784 – 796, 2007.
[22] Macdonald, M., McKay, R. J., Vasile, M., and Bosquillon de Frescheville, F., "Extension of the Sun-Synchronous Orbit", Journal of Guidance, Control, and Dynamics, Vol. 33, No. 6, pp 1935 – 1940, 2010.
[23] McInnes, C. R., McDonald, A. J. C., Simmons, J. F. L., and MacDonald, E. W., "Solar Sail Parking in Restricted Three-Body Systems", Journal of Guidance, Dynamics and Control, Vol. 17, No. 2, pp. 399-406, 1994.
[24] McKay, R. J., Macdonald, M., Bosquillon de Frescheville, F., Vasile, M., McInnes, C. R., and Biggs, J. D., "Non-Keplerian Orbits Using Low Thrust, High ISP Propulsion Systems", In 60th International Astronautical Congress, IAC Paper 09.C1.2.8, Daejeon, Republic of Korea, Oct 12 – 16, 2009.
[25] Wawrzyniak, G. G., and Howell, K. C., "The Solar Sail Lunar Relay Station: An Application of Solar Sails in the Earth-Moon System", In 59th International Astronautical Congress, IAC Paper 08.C1.3.14, Glasgow, Scotland, 29 September – 03 October 2008.
[26] McInnes, C. R., and Simmons, J. F. L., "Halo Orbits for Solar Sails: Dynamics and Applications", European Space Agency Journal, Vol. 13, No. 3, pp.229-234, 1989.
[27] Simo, J., and McInnes, C. R., "Designing Displaced Lunar Orbits Using Low Thrust Propulsion", Journal of Guidance, Control, and Dynamics, Vol. 33, No. 1, pp. 259-265, 2010.
[28] Morabito, D., and Hastrup, R., "Communications With Mars During Periods of Solar Conjunction", Aerospace Conference Proceedings, IEEE , vol.3, pp. 3-1271- 3-1281, 2002.
[29] Wallace, N., "Testing of the Qinetiq T6 Thruster in Support of the ESA BepiColombo Mercury Mission", Proceedings of the 4th International Spacecraft Propulsion Conference (ESA SP-555), Chia Laguna, Cagliari, Italy, 2 – 9 June 2004.
[30] Shambayati, S., Morabito, D., Border, J. S., Davarian, F., Lee, D., Mendoza, R., Britcliffe, M., and Weinreb, S., "Mars Reconnaissance Orbiter Ka-Band (32 GHz) Demonstration: Cruise Phase Operations", The Proceedings of the AIAA SpaceOps 2006 Conference, Rome, Italy, June 19-24, 2006.
[31] Gangale, T.. "MarsSat: Assured Communications with Mars", Annals of the New York Academy of Sciences, Vol. 1065: pp. 296-310, 2005.
[32] Strizzi, J. D., Kutrieb, J. M., Damphousse, P. E., and Carrico, J. P., "Sun-Mars Libration Points and Mars Mission Simulations", Advances in the Astronautical Sciences, Vol. 108 (1), pp. 807-822, 2001.
[33] Dachwald, B., Macdonald, M., McInnes, C. R., Mengali, G., and Quarta, A. A., "Impact of Optical Degradation on Solar Sail Mission Performance", Journal of Spacecraft and Rockets, Vol. 44, No. 4, pp. 740-749, 2007.
[34]Macdonald, M., McInnes, C.R., "Solar Sail Science Mission Applications and Advancement", submitted to a special solar sail issue of the journal Advances in Space Research, November 2010.
[35] Leipold, M., and, Götz, M., "Hybrid Photonic/Electric Propulsion", Kayser-Threde, TR SOL4-TR-KTH-0001, Munich, ESA Contract No. 15334/01/NL/PA, January 2002.
[36] Mengali, G., and Quarta, A. A., "Trajectory Design with Hybrid Low-Thrust Propulsion System", Journal of Guidance, Control, and Dynamics, Vol. 30, No. 2, pp. 419-426, 2007.
[37] Baig, S., and McInnes, C. R., "Artificial Three-Body Equilibria for Hybrid Low-Thrust Propulsion", Journal of Guidance, Control, and Dynamics, Vol. 31, No. 6, pp. 1644-1655, 2008.
[38] Ceriotti, M., and McInnes, C. R., "A Near Term Pole-Sitter Using Hybrid Solar Sail Propulsion", 2nd International Symposium on Solar Sailing, ISSS 2010, New York, July 20-22, 2010.
[39] McInnes, C. R., "Artificial Lagrange Points for a Partially Reflecting Flat Solar Sail", Journal of Guidance, Control and Dynamics, Vol. 22, No. 1, pp. 185-187, 1999.
[40] D'Accolti, G., Beltrame, G., Ferrando, E., Brambilla, L., Contini, R., Vallini, L., Mugnuolo, R., Signorini, C., Caon, A., and Fiebrich, H., "The Solar Array Photovoltaic Assembly for the Rosetta Orbiter and Lander Spacecrafts", Space Power, Proceedings of the Sixth European Conference (p.445, ESA SP-502), Porto, Portugal, 6 -10 May 2002.
[41] Racca, G. D., Marini, A., Stagnaro, L., van Dooren, J., di Napoli, L., Foing, B. H., Lumb, R., Volp, J., Brinkmann, J., Grünagel, R., Estublier, D., Tremolizzo, E., McKay, M., Camino, O., Schoemaekers, J., Hechler, M., Khan, M., Rathsman, P., Andersson, G., Anflo, K., Berge, S., Bodin, P., Edfors, A., Hussain, A., Kugelberg, J., Larsson, N., Ljung, B., Meijer, L., Mörtsell, A., Nordebäck, T., Persson, S., and Sjöberg, F., "SMART-1 Mission Description and Development Status", Planetary and Space Science, Vol. 50, Issues 14-15, pp. 1323-1337, 2002.
[42] McKay, R. J., Macdonald, M., Vasile, M., and Bosquillon de Frescheville, F., "A Novel Interplanetary Communications Relay", In AIAA/AAS Astrodynamics Specialist Conference, Toronto, Canada, Aug 2-5, 2010.

[43] Vasile, M., and Bernelli-Zazzera, F., "Targeting a Heliocentric Orbit Combining Low-Thrust Propulsion and Gravity Assist Manoeuvres", Operations Research in Space and Air, Applied Optimization, Vol. 79, Kluwer Academic, Norwell, MA, 2003.
[44] Vasile, M., and Bernelli-Zazzera, F., "Optimizing Low-Thrust and Gravity Assist Manoeuvres to Design Interplanetary Trajectories", Journal of the Astronautical Sciences, Vol. 51, No. 1, Jan.–Mar. 2003, pp. 13–35.
[45] Walker, M.J.H., Ireland, B., Owens, J., "A Set of Modified Equinoctial Elements", Celestial Mechanics, Vol. 36, 1985, pp. 409-419.
[46] Betts, J. T., "Optimal Interplanetary Orbit Transfers by Direct Transcription", Journal of Astronautical Sciences, Vol. 42, No. 3, July-Sept. 1994, pp 247-268.
[47] Pernicka, H., Henry, D., and Chan, M., "Use of Halo Orbits to Provide a Communication Link Between Earth and Mars", AIAA/AAS Astrodynamics Conference, Paper 92-4584, Hilton Head Island, South Carolina, Aug 10-12, 1992.
[48] Gurfil, P., and Meltzer, D., "Stationkeeping on Unstable Orbits: Generalization to the Elliptic Restricted Three-Body Problem", Journal of Astronautical Sciences, Vol. 54, No. 1, pp.32, 2006.